Theor. Comput. Fluid Dyn. (2007) 21: 201–229
DOI 10.1007/s00162-007-0044-3

ORIGINAL ARTICLE

Bruno Chaouat · Roland Schiestel

From single-scale turbulence models to multiple-scale and subgrid-scale models by Fourier transform

Received: 6 March 2006 / Accepted: 2 November 2006 / Published online: 14 March 2007

Abstract A theoretical method based on mathematical physics formalism that allows transposition of turbulence modeling methods from URANS (unsteady Reynolds averaged Navier–Stokes) models, to multiple-scale models and large eddy simulations (LES) is presented. The method is based on the spectral Fourier transform of the dynamic equation of the two-point fluctuating velocity correlations with an extension to the case of non-homogenous turbulence. The resulting equation describes the evolution of the spectral velocity correlation tensor in wave vector space. Then, we show that the full wave number integration of the spectral equation allows one to recover usual one-point statistical closure whereas the partial integration based on spectrum splitting gives rise to partial integrated transport models (PITM). This latter approach, depending on the type of spectral partitioning used, can yield either a statistical multiple-scale model or subfilter transport models used in LES or hybrid methods, providing some appropriate approximations are made. Closure hypotheses underlying these models are then discussed by reference to physical considerations with emphasis on identification of tensorial fluxes that represent turbulent energy transfer or dissipation. Some experiments such as the homogeneous axisymmetric contraction, the decay of isotropic turbulence, the pulsed turbulent channel flow and a wall injection induced flow are then considered as typical possible applications for illustrating the potentials of these models.

Keywords Turbulence · Mathematical turbulence modeling · Spectral modeling · Partial integrated transport models · Multiple-scale models · Subgrid-scale models

PACS 47.27E (Turbulent flows, simulation and modeling)

1 Introduction

Mathematical turbulence modeling methods have made significant progress in the past decade for predicting both internal and external turbulent flows. Many different approaches in turbulence modeling have been developed up to now, such as Reynolds-averaged Navier–Stokes (RANS) models of first- and second-order based on one-point statistical closures ranging from algebraic models to transport equation models using various types of formulations [1–3], multiple-scale models derived from two-point statistical closure [4,5], and the method of large eddy simulations [6] (LES). LES method based on subgrid modeling techniques has been now extensively developed because of the increase of computer power and speed. All these various

Communicated by S. Sarkar.

B. Chaouat (✉)
Department of Computational Fluid Dynamics, ONERA, 92322 Châtillon, France
E-mail: Bruno.Chaouat@onera.fr

R. Schiestel
CNRS, IRPHE, Château-Gombert, 13384 Marseille, France

approaches have often been developed independently and the connection between them is not always clearly established. Generally, the RANS models appear well suited to handle engineering applications involving strong effects of streamline curvature, system rotation, wall injection or adverse pressure gradient encountered for instance in aeronautics and complex flows in industry and environment [7–10]. LES models are rather applied for simulating turbulent flows in fundamental studies with a special emphasis focused on tracking turbulent flow structures, two-point velocity distribution and spectra, pressure–strain fluctuating correlations and dissipation that cannot be obtained from experiment, but also for simulating turbulent engineering flows in which a particular difficult phenomenon occurs [11]. Considering the performances and drawbacks of these two different approaches that are RANS and LES, it seems that the decision of applying one model rather than the other depends on several criteria. The choice is not only governed by the intrinsic performances of the model itself, but it depends also on the type of the physical phenomena involved and the answers that are expected to the problem. Also, the computational framework, academic or industrial, is influential. It is of interest to remark that recently new turbulence models that take advantage of RANS and LES approaches based on hybrid zonal methods [12–15] or on hybrid continuous methods with seamless coupling [16–18] have been developed for simulating engineering flows on relatively coarse grid when the spectral cutoff is located before the inertial zone of the energy spectrum. This line of thought appears to have gained major interest both from a fundamental and theoretical point of view because it bridges different levels of description as well as on the applied point of view for developing efficient practical methods [19,20]. Considering these various and numerous turbulence modeling models, developed often independently from each other, it appears that there is a need to throw a bridge between these apparently different approaches, referring to their basic physical foundations. With a particular emphasis upon the connection between RANS and LES, we shall show that useful transpositions are possible if some approximations however are conceded.

The two-point approach of non-homogeneous turbulent fields as an expansion about homogeneity is used to develop both multiple scale statistical models and subfilter transport closures. Many important works have been done in the past years on the methods to extend two-point closures and spectral closure to the case of non-homogeneous turbulence. Theses various approaches, based on two-point correlations allow one to represent all the turbulence scales and the directional properties of structures. After the work of Cambon et al. [21] dealing with the extension of EDQNM (eddy-damped quasi-normal Markovian) closures to homogeneous anisotropic turbulence, several efforts have been made to extend the method to non-homogeneous turbulence. Burden [22] was among the first attempts introducing weak inhomogeneity based on developments about homogeneity. Among these contributions also, the work of Besnard et al. [23] provides the exact equations of double correlation spectra in the case of non-homogeneous fields, used as a basis for developing non-homogenous spectral closures. Laporta and Bertoglio [24,25] derived the full equations for two-point correlations and spectra in non-homogeneous fields. But considering the high complexity of the algebra, the model was reduced to one dimension by shell integration. The variations of mean velocity in space was accounted by the use of Taylor series approximations rather than complete Fourier transform. This method is useful for introducing free flow inhomogeneity that extend in all space but the presence of walls bring new considerable complexities. These complexities are indeed reflecting the fact that Fourier transform is not the appropriate operator to apply for fully inhomogeneous fields. It can however still be very useful if some approximations are accepted. A simplified form of spectral model based on the energy spectrum has been developed by Bertoglio and Jeandel [26] and afterwards by Parpais [27] for practical applications. The extension to the one-dimensional spectral tensor of double velocity correlation has been considered by Touil et al. [28,29]. The works of Clark and Zemach [30] as well as Rubinstein and Clark [31] are also related to spectral dynamic closures based on DIA (direct interaction approximation) or on Heisenberg model, that are able to exhibit refined properties of the turbulence field. One may cite also the work of Yoshisawa [32] that introduces a two scale expansion in the DIA equations formalism. An interesting overview is also given in reference [33]. Two-point correlation equations in physical and in spectral space have also been used to develop one point statistical multiple scale models. Assuming that turbulent scales vary much faster than the mean flow field, non-local operators can be approximated in Taylor series. So that when the development is limited to a linear term, it can be interpreted has a locally tangent homogeneous space. Assuming these hypotheses, multiple scale models based of transport equations for several spectral slices have been developed by Schiestel [5,34,35]. Note that another multiscale approach based on the spectral model of Clark and Zemach [30] has been also developed by Cadiou et al. [36]. These authors have introduced several characteristic length scales that are deduced from the series of moments of the spectral one dimensional tensor.

In the present paper, we propose a theoretical method based on mathematical physics formalism that allows transposition of turbulence modeling from RANS to LES. Some efforts have been made these last

years by various authors that attempt to bridge the gap between the traditional RANS method and the LES approach, giving further insight into VLES (very large eddy simulation), as made by Liu and Shih [37], for instance. Several works in the recent literature also show that the use of more advanced model for subgrid closure, including algebraic models or stress transport models inspired from RANS may be beneficial [38,39]. This can be related also to the hybrid RANS/LES approach with seamless coupling [15,20].

Spectral turbulence theory provides the main ingredient of this development. The theory deals with the dynamic equation of the two-point velocity fluctuating correlations with extensions to the case of non-homogenous flows. This choice is motivated by the fact that the two-point velocity correlation equation enables a detailed description of the turbulence field that also contains the one point information as a special case. Then, using Fourier transform and performing averaging on spherical shells on the dynamic equation, leads formally to the evolution equation of the spectral velocity correlation tensor in one-dimensional spectral space. In this situation, the turbulence quantities are represented by functions of the scalar wave number rather than a wave vector. This spectral equation has been retained for developing one-dimensional non-isotropic spectral models [40,21,41]. On the one hand, a full integration over the wave number space of the resulting evolution equation of the spectral velocity correlation tensor allows one to recover formally usual one-point statistical models. On the other hand, a partial integration over a split spectrum, with a given spectral partitioning, yields partial integrated transport models (PITM) that can be transposed both in statistical multiple-scale models and in subfilter scale modeling for large eddy simulations [16,17]. Closure of these different transport equations needs modeling of the pressure-strain correlation, inertial and fast transfers, diffusive and dissipative processes. These physical processes are identified and discussed in spectral space. In usual turbulent flows, the spectral energy distribution is evolving in time and space and in the multiple-scale framework, the splitting wave numbers also vary accordingly. This procedure provides a clue for deriving the flux equations in statistical split spectrum models. In the case of large-eddy simulations, however, the filter width is imposed and we show how the transfer terms can be directly computed. The dissipative terms are considered equals to the corresponding spectral fluxes issuing from the last slice of the spectrum.

Some typical applications are considered for illustrating the capabilities of each turbulence model. The homogeneous axisymmetric contraction flow and the decay of isotropic turbulence with an initial perturbed spectrum are presented in the framework of multiple-scales models. LES simulations using partial integrated models for unsteady turbulent channel flow subjected to a periodic forcing or wall injection including laminar to turbulent transition regimes are then considered and briefly discussed. These concepts give rise to continuous hybrid modeling techniques.

2 Transport equation of the two-point velocity fluctuation

We consider the turbulent flow of a viscous fluid. In the present case, each flow variable is decomposed into a statistical mean value and a fluctuating turbulent part which is developed into several ranks of fluctuating parts using an extension of the Reynolds decomposition. For the velocity component, we write then

$$u_i = \langle u_i \rangle + \sum_{m=1}^{N} u_i^{'(m)}, \tag{1}$$

where the partial fluctuating velocities are defined by partial integration of their generalized Fourier transform

$$u_i^{'(m)}(\boldsymbol{\xi}) = \int\limits_{\kappa_{m-1}<|\boldsymbol{\kappa}|<\kappa_m} \widehat{u'}_i(\boldsymbol{\kappa}) \exp(j\boldsymbol{\kappa}\boldsymbol{\xi}) \mathrm{d}\boldsymbol{\kappa}, \tag{2}$$

where $\widehat{u'}_i(\boldsymbol{\kappa})$ denotes the Fourier transform of $u'_i(\boldsymbol{\xi})$ and κ_m is a series of evolving partitioning wave numbers. Applying the basic decomposition of the turbulent velocity defined by relations (1) and (2) for $m = 1$ enables one to recover the velocity decomposition $u_i = \langle u_i \rangle + u_i^{'(1)}$ used in RANS models in which the whole spectrum is modeled. For $m = 2$ or higher, we find the usual decomposition retained for the multiple-scale statistical models. The two-level decomposition $m = 2$ is also relevant for the decomposition used in large eddy simulations where only one part of the spectrum containing the small eddies is modeled $u_i = \langle u_i \rangle + u_i^{<} + u_i^{>}$ with $u_i^{<} = u_1^{(1)}$ and $u_i^{>} = u_2^{(2)}$, whereas for the other part of the spectrum containing large eddies is resolved

by the simulation. In this case, it is of interest to note that the velocity computed as $\bar{u}_i = \langle u_i \rangle + u_i^<$ represents in fact the filtered velocity which contains both statistical mean and large eddies fluctuations whereas $u_i^>$ is the subgrid-scale fluctuation of the small eddies. This definition can be viewed in fact as a special particular case of the Yoshizawa statistical filter [42,43]

$$\bar{u}_i(\boldsymbol{\xi}) = \int\limits_{|\boldsymbol{\kappa}|<\kappa_c} \hat{u}_i(\boldsymbol{\kappa}) \exp(j\boldsymbol{\kappa}\boldsymbol{\xi}) \mathrm{d}\boldsymbol{\kappa} + \left\langle \int\limits_{|\boldsymbol{\kappa}|<\kappa_c} \hat{u}_i(\boldsymbol{\kappa}) \exp(j\boldsymbol{\kappa}\boldsymbol{\xi}) \mathrm{d}\boldsymbol{\kappa} \right\rangle. \tag{3}$$

In the present case, we shall consider that the approximation of locally homogeneous anisotropic turbulence can be used, so that the statistical mean of the Fourier modes are all zero $\langle \hat{u}_i(\boldsymbol{\kappa}) \rangle = 0$ except for $\boldsymbol{\kappa} = 0$. Then, the zero mode give rise to the constant mean value $\langle u_i \rangle$ and

$$\bar{u}_i = \langle u_i \rangle + u_i^< = \langle u_i \rangle + \int\limits_{|\boldsymbol{\kappa}|<\kappa_c} \widehat{u'}_i(\boldsymbol{\kappa}) \exp(j\boldsymbol{\kappa}\boldsymbol{\xi}) \mathrm{d}\boldsymbol{\kappa}. \tag{4}$$

The approximation of tangent homogeneous field will be discussed in the remainder of the paper. It implies also that the mean value will not be Fourier transformed but is approximated by a Taylor series. One can remark, already, that the filter (4) presents the twofold interpretation of a statistical filter, in the sense that being defined as a linear combination of modes which are random variables, it is a Fourier space filter but it is also a partial statistical mean. This twofold character will be useful for RANS/LES transpositions.

The general case of non-isotropic inhomogeneous turbulence is considered in the present formalism for linking the different turbulence modeling approaches. In this case, the two-point velocity correlation $R_{ij} = \langle u'_{iA} u'_{jB} \rangle$ is function of the distance between the points A and B, denoted ξ, but also of the location of these points $\boldsymbol{x}_A$ and $\boldsymbol{x}_B$ in the flow field because of the inhomogeneity of the turbulence field. New independent variables defined by the vector difference $\boldsymbol{\xi} = \boldsymbol{x}_B - \boldsymbol{x}_A$ and the midway position $\boldsymbol{X} = \frac{1}{2}(\boldsymbol{x}_A + \boldsymbol{x}_B)$ are then introduced in the present derivation in order to distinguish the effects of distance separation from the effects of space location. So that each variable can be regarded as a function of the two variables $\boldsymbol{\xi}$ and $\boldsymbol{X}$. Taking into account these considerations, we can write the complete dynamic equation for the double velocity correlation for incompressible fluid flow as follows [44]

$$\begin{aligned}
&\frac{\partial R_{ij}(\boldsymbol{X},\boldsymbol{\xi})}{\partial t} + \frac{1}{2}\big(\langle u_{kA}\rangle + \langle u_{kB}\rangle\big)\frac{\partial R_{ij}(\boldsymbol{X},\boldsymbol{\xi})}{\partial X_k} \\
&= -R_{jk}(\boldsymbol{X},\boldsymbol{\xi})\left(\frac{\partial \langle u_i\rangle}{\partial x_k}\right)_A - R_{ik}(\boldsymbol{X},\boldsymbol{\xi})\left(\frac{\partial \langle u_j\rangle}{\partial x_k}\right)_B \\
&\quad -\big(\langle u_{kB}\rangle - \langle u_{kA}\rangle\big)\frac{\partial R_{ij}(\boldsymbol{X},\boldsymbol{\xi})}{\partial \xi_k} - \frac{1}{2}\frac{\partial}{\partial X_k}\Big(\big\langle u'_{iA}u'_{kB}u'_{jB}\big\rangle + \big\langle u'_{iA}u'_{kA}u'_{jB}\big\rangle\Big)(\boldsymbol{X},\boldsymbol{\xi}) \\
&\quad -\frac{\partial}{\partial \xi_k}\Big(\big\langle u'_{iA}u'_{kB}u'_{jB}\big\rangle - \big\langle u'_{iA}u'_{kA}u'_{jB}\big\rangle\Big)(\boldsymbol{X},\boldsymbol{\xi}) - \frac{1}{2\rho}\left(\frac{\partial}{\partial X_i}\big\langle p'_A u'_{jB}\big\rangle + \frac{\partial}{\partial X_j}\big\langle p'_B u'_{iA}\big\rangle\right)(\boldsymbol{X},\boldsymbol{\xi}) \\
&\quad +\frac{1}{\rho}\left(\frac{\partial}{\partial \xi_i}\big\langle p'_A u'_{jB}\big\rangle - \frac{\partial}{\partial \xi_j}\big\langle p'_B u'_{iA}\big\rangle\right)(\boldsymbol{X},\boldsymbol{\xi}) + \frac{\nu}{2}\frac{\partial^2 R_{ij}}{\partial X_l \partial X_l}(\boldsymbol{X},\boldsymbol{\xi}) + 2\nu\frac{\partial^2 R_{ij}}{\partial \xi_l \partial \xi_l}(\boldsymbol{X},\boldsymbol{\xi}).
\end{aligned} \tag{5}$$

The Fourier transform of this equation in the general case of non-homogenous turbulence is developed in Laporta work [24]. The main complexities arises from the production and convection terms that involve the mean velocity. This method [24] allows one to avoid the Fourier transform of the mean velocity itself. It is based on a Taylor series representation of the mean velocity such that

$$\langle u_{kB}\rangle - \langle u_{kA}\rangle \approx \xi_m \frac{\partial \langle u_k\rangle}{\partial X_m} + \cdots, \tag{6}$$

$$\langle u_{kA}\rangle + \langle u_{kB}\rangle \approx 2\langle u_k\rangle(X_m) + \frac{\xi_m \xi_p}{2}\frac{\partial^2 \langle u_k\rangle}{\partial X_m \partial X_p} + \cdots, \tag{7}$$

$$R_{jk}\left(\frac{\partial \langle u_i\rangle}{\partial x_k}\right)_A + R_{ik}\left(\frac{\partial \langle u_j\rangle}{\partial x_k}\right)_B \approx R_{jk}\frac{\partial \langle u_i\rangle}{\partial X_k} + R_{ik}\frac{\partial \langle u_j\rangle}{\partial X_k} - \frac{\xi_m}{2}R_{jk}\frac{\partial^2 \langle u_i\rangle}{\partial X_k \partial X_m} + \frac{\xi_m}{2}R_{ik}\frac{\partial^2 \langle u_i\rangle}{\partial X_k \partial X_m} + \cdots . \tag{8}$$

Then, if the development is restricted to its first term only, then $\langle u_k\rangle (X_m + \xi_m) = \langle u_k\rangle (X_m) + \Lambda_{kj}\xi_j$, and the Fourier terms are identical to the ones in homogeneous anisotropic turbulence. This approach is equivalent to consider that the mean velocity gradient is locally "constant". The complete equation in physical space which contains additive contributions of homogeneous and non-homogenous terms can be written in the following way:

$$\begin{aligned}
&\frac{\partial R_{ij}(\boldsymbol{X},\boldsymbol{\xi})}{\partial t} + \langle u_k\rangle \frac{\partial R_{ij}(\boldsymbol{X},\boldsymbol{\xi})}{\partial X_k} \\
&= -R_{jk}(\boldsymbol{X},\boldsymbol{\xi})\frac{\partial \langle u_i\rangle}{\partial X_k} - R_{ik}(\boldsymbol{X},\boldsymbol{\xi})\frac{\partial \langle u_j\rangle}{\partial X_k} \\
&\quad - \xi_p \frac{\partial \langle u_k\rangle}{\partial X_p}\frac{\partial R_{ij}}{\partial \xi_k}(\boldsymbol{X},\boldsymbol{\xi}) - \frac{1}{2}\frac{\partial}{\partial X_k}(S_{i,kj} - S_{ik,j})(\boldsymbol{X},\boldsymbol{\xi}) - \frac{\partial}{\partial \xi_k}(S_{i,kj} - S_{ik,j})(\boldsymbol{X},\boldsymbol{\xi}) \\
&\quad - \frac{1}{2\rho}\left(\frac{\partial K_{(p)j}}{\partial X_i} + \frac{\partial K_{i(p)}}{\partial X_j}\right)(\boldsymbol{X},\boldsymbol{\xi}) + \frac{1}{\rho}\left(\frac{\partial K_{(p)j}}{\partial \xi_i} - \frac{\partial K_{i(p)}}{\partial \xi_j}\right)(\boldsymbol{X},\boldsymbol{\xi}) \\
&\quad + \frac{\nu}{2}\frac{\partial^2 R_{ij}(\boldsymbol{X},\boldsymbol{\xi})}{\partial X_l \partial X_l} + 2\nu\frac{\partial^2 R_{ij}(\boldsymbol{X},\boldsymbol{\xi})}{\partial \xi_l \partial \xi_l},
\end{aligned} \tag{9}$$

where the term $S_{i,jk}$ and $S_{ik,j}$ denote the turbulent diffusion terms due to the fluctuating velocities

$$\begin{aligned}
S_{i,kj}(\boldsymbol{X},\boldsymbol{\xi}) &= \left\langle u'_{i_A} u'_{k_B} u'_{j_B}\right\rangle, \\
S_{ik,j}(\boldsymbol{X},\boldsymbol{\xi}) &= \left\langle u'_{i_A} u'_{k_A} u'_{j_B}\right\rangle,
\end{aligned} \tag{10}$$

and the terms $K_{(p)i}$ and $K_{i(p)}$ are turbulent diffusion terms due to the fluctuating pressure defined by

$$K_{(p)i}(\boldsymbol{X},\boldsymbol{\xi}) = \left\langle p'_A u'_{i_B}\right\rangle, \tag{11}$$

and

$$K_{i(p)}(\boldsymbol{X},\boldsymbol{\xi}) = \left\langle p'_B u'_{i_A}\right\rangle. \tag{12}$$

Note that $K_{(p)i}(\boldsymbol{X},\boldsymbol{\xi}) = K_{i(p)}(\boldsymbol{X},-\boldsymbol{\xi})$, and $K_{(p)i}(\boldsymbol{X},\boldsymbol{\xi}) = -K_{(p)i}(\boldsymbol{X},-\boldsymbol{\xi})$. This is demonstrated in detail in reference [44]. In Eq. (9), we have chosen the analytic form, which gives a direct connection with the one-point Reynolds stress equation [5,40]. In particular, we emphasize that Taylor series expansion in space have been applied for computing the velocity at different points. So, the mean velocity field will not be the Fourier transformed but is rather approximated by a Taylor series. As mentioned by Schiestel [5], the non-homogenous terms that appear in Eq. (9) correspond to the usual terms in one-point equation whereas the others terms involving the distance ξ can be treated as in homogeneous anisotropic turbulence. Therefore, this method can be viewed as considering the tangent homogeneous anisotropic field at point $\boldsymbol{X}$ of the non-homogenous field. This useful concept will be used throughout the paper. It is based on the idea that a locally tangent homogeneous turbulence field can be defined by analytic continuation from the knowledge of derivative of correlations at $\boldsymbol{\xi} = 0$. More precisely, the knowledge of $\partial_{ij\ldots m}C(\boldsymbol{\xi} = 0)$ where C is a statistical correlation is thus equivalent to the knowledge of the spectrum $\widehat{C}(\boldsymbol{\kappa})$, rebuilt from its moments

$$\int \kappa_i \kappa_j \cdots \kappa_m \widehat{C}(\boldsymbol{\kappa})\mathrm{d}\boldsymbol{\kappa}. \tag{13}$$

Indeed, this approach encounters difficulties when wall boundaries are introduced [24] because Fourier transform is no longer the appropriate mathematical tool. In this case, the equations can still be considered formally

and empirically adapted to account for wall effects. Considering the Fourier transform of $R_{ij}(\boldsymbol{X},\boldsymbol{\xi})$ that is expressed as

$$\widehat{R}_{ij}(\boldsymbol{X},\boldsymbol{\kappa}) = \int R_{ij}(\boldsymbol{X},\boldsymbol{\xi}) \exp\left(-j\boldsymbol{\kappa}\boldsymbol{\xi}\right) \mathrm{d}\boldsymbol{\xi}, \tag{14}$$

the transport equation of the double velocity correlation in locally tangent spectral space then reads

$$\begin{aligned}
&\frac{\partial \widehat{R}_{ij}(\boldsymbol{X},\boldsymbol{\kappa})}{\partial t} + \langle u_k\rangle \frac{\partial \widehat{R}_{ij}(\boldsymbol{X},\boldsymbol{\kappa})}{\partial X_k} \\
&= -\widehat{R}_{jk}(\boldsymbol{X},\boldsymbol{\kappa}) \frac{\partial \langle u_i\rangle}{\partial X_k} - \widehat{R}_{ik}(\boldsymbol{X},\boldsymbol{\kappa}) \frac{\partial \langle u_j\rangle}{\partial X_k} \\
&\quad + \kappa_k \frac{\partial \langle u_k\rangle}{\partial X_p} \frac{\partial \widehat{R}_{ij}}{\partial \kappa_p}(\boldsymbol{X},\boldsymbol{\kappa}) - \frac{1}{2}\frac{\partial}{\partial X_k}(\widehat{S}_{i,kj} + \widehat{S}_{ik,j})(\boldsymbol{X},\boldsymbol{\kappa}) - j\kappa_k(\widehat{S}_{i,kj} - \widehat{S}_{ik,j})(\boldsymbol{X},\boldsymbol{\kappa}) \\
&\quad - \frac{1}{2\rho}\left(\frac{\partial \widehat{K}_{(p)j}}{\partial X_i} + \frac{\partial \widehat{K}_{i(p)}}{\partial X_j}\right)(\boldsymbol{X},\boldsymbol{\kappa}) + \frac{j}{\rho}\left(\kappa_i\, \widehat{K}_{(p)j} - \kappa_j\, \widehat{K}_{i(p)}\right)(\boldsymbol{X},\boldsymbol{\kappa}) \\
&\quad + \frac{\nu}{2}\frac{\partial^2 \widehat{R}_{ij}(\boldsymbol{X},\boldsymbol{\kappa})}{\partial X_l \partial X_l} - 2\nu\kappa^2 \widehat{R}_{ij}(\boldsymbol{X},\boldsymbol{\kappa}).
\end{aligned} \tag{15}$$

Referring to the work of Besnard et al. [23], this equation appears as a first order approximation of the exact spectral transport equations. Pressure terms can be calculated from the Poisson equations obtained by applying the divergence operator to the double correlation equations [25,44,45].

3 One-dimensional models by spherical mean

For each variable $f(\boldsymbol{x})$ and its Fourier transform $\hat{f}(\boldsymbol{\kappa})$, we define the spherical mean of the Fourier transform by the relation

$$(f(\boldsymbol{x}))^{\Delta} = f^{\Delta}(\kappa) = \frac{1}{A(\kappa)} \int\!\!\int_{\partial A} \hat{f}(\boldsymbol{\kappa}) \mathrm{d}A(\boldsymbol{\kappa}), \tag{16}$$

where $\mathrm{d}A(\boldsymbol{\kappa})$ is the area element on the sphere of radius $\kappa = |\boldsymbol{\kappa}|$. The transport equation of the one-dimensional spectral tensor of the double velocity correlations, which governs the turbulent processes which develop in the one-dimensional Fourier space, is obtained by taking the Fourier transform and mean integration over spherical shells of original Eq. (15) in physical space. Spherical averages allow one to make some useful simplifications in the spectral equations, loosing the directional information, the averaged spectral correlations are then only function of the wavenumber and not any more of the wavevector. This practice has been currently used in the Lyon group in France [21,26,28,29]. Remaining within the framework of the tangent homogeneous spectral space, this equation then reads

$$\begin{aligned}
&\frac{\partial \varphi_{ij}}{\partial t}(\boldsymbol{X},\kappa) + \langle u_k\rangle \frac{\partial \varphi_{ij}(\boldsymbol{X},\kappa)}{\partial X_k} \\
&= \mathcal{P}_{ij}(\boldsymbol{X},\kappa) + \theta_{ij}(\boldsymbol{X},\kappa) + \zeta_{kimj}(\boldsymbol{X},\kappa)\frac{\partial \langle u_k\rangle}{\partial X_m} \\
&\quad + \Xi_{ij}(\boldsymbol{X},\kappa) - \frac{1}{2}\frac{\partial}{\partial X_k}\left(\varsigma_{i,kj} + \varsigma_{ik,j}\right)(\boldsymbol{X},\kappa) + \Upsilon_{ij}(\boldsymbol{X},\kappa),
\end{aligned} \tag{17}$$

where the function φ_{ij} denotes the spherical mean of the Fourier transform of the two-point correlation tensor

$$\varphi_{ij}(\boldsymbol{X},\kappa) = \left(R_{ij}(\boldsymbol{X},\boldsymbol{\xi})\right)^{\Delta}. \tag{18}$$

This type of approach is the basis of spectral models developed in references [21,40]. On the right-hand side of Eq. (17), $\mathcal{P}_{ij}$ represents the production term defined by

$$\mathcal{P}_{ij}(\boldsymbol{X},\kappa) = -\varphi_{ik}(\boldsymbol{X},\kappa)\frac{\partial\left\langle u_j\right\rangle}{\partial X_k} - \varphi_{jk}(\boldsymbol{X},\kappa)\frac{\partial\left\langle u_i\right\rangle}{\partial X_k}, \tag{19}$$

the first transfer term θ_{ij} related to the triple velocity correlations, is the inertial cascade

$$\theta_{ij}(\boldsymbol{X},\kappa) = -\left(\frac{\partial}{\partial\xi_k}\left(S_{i,kj} - S_{ik,j}\right)(\boldsymbol{X},\boldsymbol{\xi})\right)^{\Delta}, \tag{20}$$

the second transfer term ζ_{kimj} represents the fast transfer by action of mean velocity gradients

$$\zeta_{kimj}(\boldsymbol{X},\kappa) = -\left(\xi_m\frac{\partial R_{ij}}{\partial\xi_k}(\boldsymbol{X},\boldsymbol{\xi})\right)^{\Delta}, \tag{21}$$

the turbulent diffusion terms $\varsigma_{i,jk}$ and $\varsigma_{ik,j}$ are due to fluctuating velocities

$$\begin{aligned}\varsigma_{i,kj}(\boldsymbol{X},\kappa) &= \left(S_{i,kj}(\boldsymbol{X},\boldsymbol{\xi})\right)^{\Delta},\\ \varsigma_{ik,j}(\boldsymbol{X},\kappa) &= \left(S_{ik,j}(\boldsymbol{X},\boldsymbol{\xi})\right)^{\Delta},\end{aligned} \tag{22}$$

the pressure terms in Eq. (17) are obtained as

$$\Xi_{ij}(\boldsymbol{X},\kappa) = \frac{1}{\rho}\left(\frac{\partial\mathcal{K}_j}{\partial\xi_i} - \frac{\partial\mathcal{K}_i}{\partial\xi_j}\right) - \frac{1}{2\rho}\left(\frac{\partial\mathcal{K}_j}{\partial X_i} + \frac{\partial\mathcal{K}_i}{\partial X_j}\right), \tag{23}$$

where $\mathcal{K}_i$ is the turbulent diffusion due to fluctuating pressure defined by

$$\mathcal{K}_i(\boldsymbol{X},\kappa) = \left(K_{i(p)}(\boldsymbol{X},\boldsymbol{\xi})\right)^{\Delta} = \left(K_{(p)i}(\boldsymbol{X},\boldsymbol{\xi})\right)^{\Delta} \tag{24}$$

Equation (24) makes use of the properties given in preceding section (2). The $\mathcal{K}_i$ term appears through its gradient in X_i in the general transport equation of the spectral tensor and consequently can be interpreted as a contribution of pressure to the turbulent diffusion. According to the present choice of independent variables, and in agreement with the one-point Reynolds stress equations deduced from the integration of Eq. (17), the following splitting is introduced [45]

$$\Xi_{ij}(\boldsymbol{X},\kappa) = \Pi_{ij}(\boldsymbol{X},\kappa) - \frac{1}{\rho}\left(\frac{\partial\mathcal{K}_j}{\partial X_i} + \frac{\partial\mathcal{K}_i}{\partial X_j}\right) \tag{25}$$

with

$$\Pi_{ij}(\boldsymbol{X},\kappa) = \frac{1}{\rho}\left(\frac{\partial\mathcal{K}_j}{\partial\xi_i} - \frac{\partial\mathcal{K}_i}{\partial\xi_j}\right) + \frac{1}{2\rho}\left(\frac{\partial\mathcal{K}_j}{\partial X_i} + \frac{\partial\mathcal{K}_i}{\partial X_j}\right), \tag{26}$$

which satisfies the condition $\Pi_{ii} = 0$ in homogeneous turbulence because of the continuity equation. The right-hand side of Eq. (25), thus, embodies two physical processes: first is the pressure-strain correlation effect and second is the turbulent diffusion effect.

The term Υ_{ij} embodies all the viscous terms, including molecular diffusion and viscous dissipation rate

$$\Upsilon_{ij}(\boldsymbol{X},\kappa) = \frac{\nu}{2}\frac{\partial^2\varphi_{ij}(\boldsymbol{X},\kappa)}{\partial X_l\partial X_l} - 2\nu\kappa^2\varphi_{ij}(\boldsymbol{X},\kappa). \tag{27}$$

The form of this term is a consequence of Fourier transform along with the particular choice of variable change introduced in paragraph 2. This splitting is different from what would be guessed from physical intuition. For this reason, we prefer to introduce the equivalent splitting

$$\Upsilon_{ij}(\boldsymbol{X},\kappa) = \nu\frac{\partial^2\varphi_{ij}(\boldsymbol{X},\kappa)}{\partial X_l\partial X_l} - \mathcal{E}_{ij}(\boldsymbol{X},\kappa), \tag{28}$$

which is consistent with the one point usual transport equation of the Reynolds stresses. The first term in the right-hand side of Eq. (28) is the molecular viscous diffusion term and the second term $\mathcal{E}_{ij}$ represents the dissipation rate

$$\mathcal{E}_{ij}(\boldsymbol{X},\kappa) = \frac{\nu}{2}\frac{\partial^2 \varphi_{ij}(\boldsymbol{X},\kappa)}{\partial X_l X_l} + 2\nu\kappa^2 \varphi_{ij}(\boldsymbol{X},\kappa), \tag{29}$$

which is now composed of two different contributions (see also a remark given by Jones and Launder [46]). Equation (29) defines the dissipation rate in the general case of non-homogeneous turbulence. For the scalar dissipation rate, this implies

$$\mathcal{E}(\boldsymbol{X},\kappa) = \frac{\nu}{2}\frac{\partial^2 E(\boldsymbol{X},\kappa)}{\partial X_l X_l} + 2\nu\kappa^2 E(\boldsymbol{X},\kappa) \tag{30}$$

with

$$E(\boldsymbol{X},\kappa) = \frac{1}{2}\varphi_{jj}(\boldsymbol{X},\kappa). \tag{31}$$

These relations have been also considered in the work of Jovanovic et al. [47] and Jakirlic and Hanjalic [48] who introduce the homogeneous dissipation rate

$$\mathcal{E}^h(\boldsymbol{X},\kappa) = \mathcal{E}(\boldsymbol{X},\kappa) - \frac{\nu}{2}\frac{\partial^2 E(\boldsymbol{X},\kappa)}{\partial X_l X_l} \tag{32}$$

in the near wall modeling. For homogeneous turbulence, the definitions for Π_{ij} in Eq. (26) and $\mathcal{E}_{ij}$ in Eq. (29) reduce to the following form

$$\Pi_{ij}(\boldsymbol{X},\kappa) = \Pi^h_{ij}(\boldsymbol{X},\kappa) = \frac{1}{\rho}\left(\frac{\partial \mathcal{K}_j}{\partial \xi_i} - \frac{\partial \mathcal{K}_i}{\partial \xi_j}\right) \tag{33}$$

and

$$\mathcal{E}_{ij}(\boldsymbol{X},\kappa) = \mathcal{E}^h_{ij}(\boldsymbol{X},\kappa) = 2\nu\kappa^2 \varphi_{ij}(\boldsymbol{X},\kappa). \tag{34}$$

We will verify in the next section that expressions for the pressure–strain correlation term as well as for the dissipation rate indeed correspond to the usual definitions used in one-point statistical models. For the clarity of the presentation, Eq. (17) is rewritten in a more compact form

$$\frac{D\varphi_{ij}(\boldsymbol{X},\kappa)}{Dt} = \mathcal{P}_{ij}(\boldsymbol{X},\kappa) + \mathcal{T}_{ij}(\boldsymbol{X},\kappa) + \Pi_{ij}(\boldsymbol{X},\kappa) + \mathcal{J}_{ij}(\boldsymbol{X},\kappa) - \mathcal{E}_{ij}(\boldsymbol{X},\kappa) \tag{35}$$

with the definition

$$\frac{D\varphi_{ij}(\boldsymbol{X},\kappa)}{Dt} = \frac{\partial \varphi_{ij}(\boldsymbol{X},\kappa)}{\partial t} + \langle u_k \rangle (\boldsymbol{X})\frac{\partial \varphi_{ij}(\boldsymbol{X},\kappa)}{\partial X_k}. \tag{36}$$

In this equation, $\mathcal{T}_{ij}$ is the total transfer term defined by

$$\mathcal{T}_{ij}(\boldsymbol{X},\kappa) = \theta_{ij}(\boldsymbol{X},\kappa) + \zeta_{kimj}(\boldsymbol{X},\kappa)\frac{\partial \langle u_k \rangle}{\partial X_m}, \tag{37}$$

and $\mathcal{J}_{ij}$ embodies all the diffusion like terms

$$\mathcal{J}_{ij}(\boldsymbol{X},\kappa) = -\frac{1}{\rho}\left(\frac{\partial \mathcal{K}_j}{\partial X_i} + \frac{\partial \mathcal{K}_i}{\partial X_j}\right) - \frac{1}{2}\frac{\partial}{\partial X_k}\left(\varsigma_{i,kj} + \varsigma_{ik,j}\right) + \nu\frac{\partial^2 \varphi_{ij}(\boldsymbol{X},\kappa)}{\partial X_l X_l}. \tag{38}$$

4 Integration in the spectral space

4.1 Full integration in spectral space for usual one-point statistical turbulence models

The full integration in the spectral space of Eq. (17) allows one to recover usual one-point statistical models in the physical space. Indeed, it corresponds to the limiting case in which the distance between the two-points goes to zero ($\xi = 0$) in physical space. The usual one-point turbulent stress tensor R_{ij} is computed as follows

$$R_{ij} = \int_0^\infty \varphi_{ij}(\boldsymbol{X}, \kappa)\mathrm{d}\kappa. \tag{39}$$

The production term P_{ij} is simply calculated from Eq. (19)

$$P_{ij} = \int_0^\infty \mathcal{P}_{ij}(\boldsymbol{X}, \kappa)\mathrm{d}\kappa = -R_{ik}\frac{\partial \langle u_j \rangle}{\partial x_k} - R_{jk}\frac{\partial \langle u_i \rangle}{\partial x_k}. \tag{40}$$

The calculation of the pressure–strain correlation is quite difficult because of the presence of several terms in Eq. (26). However, using the reciprocal change in variables for evaluating the gradients (cf. Appendix A1) allows one to obtain the usual expression

$$\Psi_{ij} = \int_0^\infty \Pi_{ij}(\boldsymbol{X}, \kappa)\mathrm{d}\kappa = \left\langle \frac{p'}{\rho}\left(\frac{\partial u_i'}{\partial x_j} + \frac{\partial u_j'}{\partial x_i}\right)\right\rangle. \tag{41}$$

The dissipation rate ϵ_{ij} is obtained by integrating the tensor $\mathcal{E}_{ij}$ defined in Eq. (29) in the spectral space. By developing the calculation (cf. Appendix A2), we finally get the usual expression of the dissipation-rate

$$\epsilon_{ij} = \int_0^\infty \mathcal{E}_{ij}(\boldsymbol{X}, \kappa)\mathrm{d}\kappa = 2\nu\left\langle \frac{\partial u_i'}{\partial x_m}\frac{\partial u_j'}{\partial x_m}\right\rangle. \tag{42}$$

The diffusion term J_{ij} computed from Eq. (38) requires also some algebra (cf. Appendix A3) to give

$$J_{ij} = \int_0^\infty \mathcal{J}_{ij}(\boldsymbol{X}, \kappa)\mathrm{d}\kappa = -\frac{1}{\rho}\left(\frac{\partial}{\partial x_i}\left\langle p'u_j'\right\rangle + \frac{\partial}{\partial x_j}\left\langle p'u_i'\right\rangle\right) - \frac{\partial}{\partial x_k}\left\langle u_i'u_j'u_k'\right\rangle + \nu\frac{\partial^2 R_{ij}}{\partial x_l x_l}. \tag{43}$$

As expected, the total transfer term T_{ij} that corresponds to the integration of the term $\mathcal{T}_{ij}$ defined in Eq. (37) vanishes because of the one-point correlations properties (cf. Appendix A4)

$$T_{ij} = \int_0^\infty \mathcal{T}_{ij}(\boldsymbol{X}, \kappa)\mathrm{d}\kappa = 0. \tag{44}$$

From the results of Eqs. (40), (41), (42), (43), (44), one can see that the present mathematical formalism provides therefore a direct connection between spectral tensor equations and the usual one-point transport equation of the turbulent Reynolds stress

$$\frac{\mathrm{D}R_{ij}}{\mathrm{D}t} = P_{ij} + \Psi_{ij} + J_{ij} - \epsilon_{ij} \tag{45}$$

whereas a tensorial contraction of Eq. (45), yields the transport equation of the turbulent kinetic energy

$$\frac{\mathrm{D}k}{\mathrm{D}t} = P + J - \epsilon. \tag{46}$$

4.2 Partial integration in spectral space for statistical multiple-scale turbulence models

The transport equation of the partial turbulent stress $R_{ij}^{(m)}$ is obtained by partial integration of the spectral spectrum in the wave number range $[\kappa_{m-1}, \kappa_m]$. The partial turbulent stress $R_{ij}^{(m)}$ is defined by

$$R_{ij}^{(m)} = \int_{\kappa_{m-1}}^{\kappa_m} \varphi_{ij}(\boldsymbol{X}, \kappa) \mathrm{d}\kappa. \tag{47}$$

Keeping in mind that the wave numbers are evolving in time, integration of Eq. (35) over the range $[\kappa_{m-1}, \kappa_m]$ provides the transport equation for the partial turbulent stress $R_{ij}^{(m)}$

$$\frac{\mathrm{D}R_{ij}^{(m)}}{\mathrm{D}t} = P_{ij}^{(m)} + F_{ij}^{(m-1)} - F_{ij}^{(m)} + \Psi_{ij}^{(m)} + J_{ij}^{(m)} - \epsilon_{ij}^{(m)}, \tag{48}$$

where

$$P_{ij}^{(m)} = \int_{\kappa_{m-1}}^{\kappa_m} \mathcal{P}_{ij}(\boldsymbol{X}, \kappa) \mathrm{d}\kappa = -R_{ik}^{(m)} \frac{\partial \langle u_j \rangle}{\partial x_k} - R_{jk}^{(m)} \frac{\partial \langle u_i \rangle}{\partial x_k}, \tag{49}$$

$$F_{ij}^{(m)} = \mathcal{F}_{ij}^{(m)} - \varphi_{ij}(\boldsymbol{X}, \kappa) \frac{\partial \kappa_m}{\partial t}, \tag{50}$$

$$\mathcal{F}_{ij}^{(m)} = -\int_{0}^{\kappa_m} \mathcal{T}_{ij}(\boldsymbol{X}, \kappa) \mathrm{d}\kappa, \tag{51}$$

and

$$\Psi_{ij}^{(m)} = \int_{\kappa_{m-1}}^{\kappa_m} \Pi_{ij}(\boldsymbol{X}, \kappa) \mathrm{d}\kappa, \tag{52}$$

$$J_{ij}^{(m)} = \int_{\kappa_{m-1}}^{\kappa_m} \mathcal{J}_{ij}(\boldsymbol{X}, \kappa) \mathrm{d}\kappa, \tag{53}$$

$$\epsilon_{ij}^{(m)} = \int_{\kappa_{m-1}}^{\kappa_m} \mathcal{E}_{ij}(\boldsymbol{X}, \kappa) \mathrm{d}\kappa. \tag{54}$$

The transport equation of the partial turbulent kinetic energy $k^{(m)}$ is simply obtained by contracting the indices of Eq. (48)

$$\frac{\mathrm{D}k^{(m)}}{\mathrm{D}t} = P^{(m)} + F^{(m-1)} - F^{(m)} + J^{(m)} - \epsilon^{(m)} \tag{55}$$

with the following definitions

$$F^{(m)} = \mathcal{F}^{(m)} - E(\boldsymbol{X}, \kappa) \frac{\partial \kappa_m}{\partial t}, \tag{56}$$

where $E(\boldsymbol{X}, \kappa) = \frac{1}{2}\varphi_{ii}(\boldsymbol{X}, \kappa)$ and $P^{(m)} = \frac{1}{2}P_{ii}^{(m)}$, $F^{(m)} = \frac{1}{2}F_{ii}^{(m)}$, $J^{(m)} = \frac{1}{2}J_{ii}^{(m)}$, $\epsilon^{(m)} = \frac{1}{2}\epsilon_{ii}^{(m)}$. On a schematic point of view, equilibrium high Reynolds number turbulence is attained when all the contributions $\epsilon_{ij}^{(m)}$ are reduced to zero in all the wave number ranges $[\kappa_{m-1}, \kappa_m]$ except for the last one (the dissipation range), which verifies the relation $\epsilon_{ij}^{(m+1)} = F_{ij}^{(m)}$.

4.3 Practical case of two-scale turbulence models

The turbulent stress in the range $[\kappa_1, \kappa_2]$ is denoted $R_{ij}^{(2)}$ and is defined by the integration of the spectral tensor $\varphi_{ij}(\boldsymbol{X}, \kappa)$ over the range domain $[\kappa_1, \kappa_2]$

$$R_{ij}^{(2)} = \int_{\kappa_1}^{\kappa_2} \varphi_{ij}(\boldsymbol{X}, \kappa) \mathrm{d}\kappa. \tag{57}$$

It is considered that the energy contained in the range of wave numbers $[\kappa_2, \infty[$ is entirely negligible. The general Eq. (48) can be applied in particular to any wave number range such as $[0, \kappa_1]$, $[\kappa_1, \kappa_2]$ and $[\kappa_2, \infty[$. Taking into account the significant processes which develop in the spectral space, one can easily obtain the resulting approximated equations

$$\frac{\mathrm{D}R_{ij}^{(1)}}{\mathrm{D}t} = P_{ij}^{(1)} - F_{ij}^{(1)} + \Psi_{ij}^{(1)} + J_{ij}^{(1)} - \epsilon_{ij}^{(1)}, \tag{58}$$

$$\frac{\mathrm{D}R_{ij}^{(2)}}{\mathrm{D}t} = P_{ij}^{(2)} + F_{ij}^{(1)} - F_{ij}^{(2)} + \Psi_{ij}^{(2)} + J_{ij}^{(2)} - \epsilon_{ij}^{(2)}, \tag{59}$$

$$0 = F_{ij}^{(2)} - \epsilon_{ij}^{(3)}, \tag{60}$$

where at high Reynolds number, we can consider that $\epsilon_{ij}^{(1)} = \epsilon_{ij}^{(2)} \approx 0$, $\epsilon_{ij}^{(3)} \approx \epsilon_{ij}$, $F_{ij}^{(1)} = F_{ij}(\kappa_1)$ and $F_{ij}^{(2)} = F_{ij}(\kappa_2)$. Equation (60) indicates that the dissipation rate ϵ can indeed be interpreted as a spectral flux. Taking into account these relations, we can write Eq. (59) in the more usual form

$$\frac{\mathrm{D}R_{ij}^{(2)}}{\mathrm{D}t} = P_{ij}^{(2)} + F_{ij}^{(1)} + \Psi_{ij}^{(2)} + J_{ij}^{(2)} - \epsilon_{ij} \tag{61}$$

with the definitions

$$P_{ij}^{(2)} = \int_{\kappa_1}^{\kappa_2} \mathcal{P}_{ij}(\boldsymbol{X}, \kappa) \mathrm{d}\kappa = -R_{ik}^{(2)} \frac{\partial \langle u_j \rangle}{\partial x_k} - R_{jk}^{(2)} \frac{\partial \langle u_i \rangle}{\partial x_k}, \tag{62}$$

$$\Psi_{ij}^{(2)} = \int_{\kappa_1}^{\kappa_2} \Pi_{ij}(\boldsymbol{X}, \kappa) \mathrm{d}\kappa, \tag{63}$$

$$J_{ij}^{(2)} = \int_{\kappa_1}^{\kappa_2} \mathcal{J}_{ij}(\boldsymbol{X}, \kappa) \mathrm{d}\kappa \tag{64}$$

and where the terms $F_{ij}^{(j)}$ and $\mathcal{F}_{ij}^{(j)}$ are given by previous Eqs. (50) and (51), respectively. Equation of the fine grained energy denoted $k^{(2)}$ is then obtained by tensor contraction of Eq. (61) over its indices, so that we obtain

$$\frac{\mathrm{D}k^{(2)}}{\mathrm{D}t} = P^{(2)} + F^{(1)} + J^{(2)} - \epsilon. \tag{65}$$

5 The need of closures hypothesis

5.1 The pressure–strain correlation terms

As in standard one-point Reynolds stress models, the pressure–strain correlation term Ψ_{ij} plays an essential role in redistributing the energy among the Reynolds stress components [49]. This term is decomposed into a slow and a rapid part that characterize the return to isotropy

$$\Psi_{ij} = \Psi_{ij}^{1} + \Psi_{ij}^{2} \tag{66}$$

where the non-linear interactions term Ψ_{ij}^1 describes action of turbulence on itself

$$\Psi_{ij}^1 = -c_1 \frac{\epsilon}{k} \left(R_{ij} - \frac{2}{3} k \delta_{ij} \right), \tag{67}$$

whereas the linear term Ψ_{ij}^2 describes the action of mean velocity gradients

$$\Psi_{ij}^2 = -c_2 \left(P_{ij} - \frac{2}{3} P \delta_{ij} \right) \tag{68}$$

The quantities c_1 and c_2 are two coefficient functions that may depend on the invariants of the anisotropy tensor defined by $a_{ij} = (R_{ij} - 2/3k\delta_{ij})/k$. Note that expressions (67) and (68) are the basic modeling used in standard RSM models, but in the past decade, more sophisticated closures have been developed in the literature [2,3,50]. The closure proposed in multiple-scale models [5] consists of applying locally Eqs. (67) and (68) in a particular spectral slice defined by the range $[\kappa_{m-1}, \kappa_m]$. For each slice contribution $\Psi_{ij}^{(m)}$ and $\Psi_{ij}^{(m,1)}$, extension of Eqs. (67) and (68) is written in the following way

$$\Psi_{ij}^{(m,1)} = -c_1^{(m)} \frac{F^{(m)}}{k^{(m)}} \left(R_{ij}^{(m)} - \frac{2}{3} k^{(m)} \delta_{ij} \right), \tag{69}$$

$$\Psi_{ij}^{(m,2)} = -c_2^{(m)} \left(P_{ij}^{(m)} - \frac{2}{3} P^{(m)} \delta_{ij} \right), \tag{70}$$

where in these expressions, the spectral flux $F^{(m)}$ is now introduced instead of the dissipation rate ϵ. Each spectral slice (m) is characterized by the quantities $F^{(m)}$ and $R_{ij}^{(m)}$. As it can be intuitively justified, the spectral flux $F^{(m)}$ which embodies several mechanisms is chosen to build the time scale because it is sensitive to the location of the spectral splitting. Considering for instance the self similar decay of grid turbulence in the initial period [34,35], the partial energy equations

$$\frac{\mathrm{d}k^{(1)}}{\mathrm{d}t} = -F^{(1)} \tag{71}$$

$$\frac{\mathrm{d}k^{(2)}}{\mathrm{d}t} = F^{(1)} - F^{(2)} \tag{72}$$

together with $F^{(2)} \approx \epsilon$, imply

$$\frac{k^{(1)}}{F^{(1)}} = \frac{k^{(2)}}{\epsilon - F^{(1)}} \tag{73}$$

using the hypothesis

$$\frac{\mathrm{d}k^{(1)}}{k^{(1)}} = \frac{\mathrm{d}k^{(2)}}{k^{(2)}} = \frac{\mathrm{d}k}{k}, \quad k = k^{(1)} + k^{(2)} \tag{74}$$

of a similar decay. Consequently,

$$\frac{F^{(1)}}{\epsilon} = \frac{k^{(1)}}{k} \tag{75}$$

The corresponding scale varies according to the ratio of partial kinetic energy. Moreover, in order to increase the return to isotropy for high wave numbers, the coefficient $c_1^{(m)}$ is no longer considered as a constant but is now dependent on the spectral slice. It increases versus the wave number κ. The specific values may be chosen empirically by reference to experimental behaviours (see for instance paragraph on the application of two and three-scale stress models). On the other hand, the coefficient $c_2^{(m)}$ is still taken as a constant. Note that these type of models can also be deduced from a spectral calculation of the term Π_{ij}^h which is defined in Eq. (33), as indicated in references [5,40].

5.2 The transfer terms

The spectral energy transfer terms appear in the transport Eqs. (48) and (59) respectively for the multiple-scale models and two-scale models as a consequence of two-point statistics. These terms need to be modeled. In this case, it is necessary to define the partitioning wave numbers through the spectrum. Indeed, because of the evolution of the turbulent characteristic scale and energy distribution in time and space, it is assumed that the splitting wave numbers are related to the local parameters $k^{(m)}$ and $F^{(m)}$ by the dimensional relation

$$\kappa_m - \kappa_{m-1} = \alpha_m \frac{F^{(m)}}{(k^{(m)})^{3/2}}, \tag{76}$$

where α_m is a numerical constant. This practice allows the splitting location to remain meaningful because it complies with the spectrum changes. The derivative of Eq. (76) with respect to time using both Eqs. (56) and (55) for evaluating the derivatives of the splitting wave number $\kappa^{(m)}$ and the partial energy $k^{(m)}$, respectively, provides the equation of the spectral flux

$$\frac{\mathrm{d}F^{(m)}}{\mathrm{d}t} = \mathcal{C}_1^{(m)} \frac{F^{(m)} P^{(m)}}{k^{(m)}} + \mathcal{C}_2^{(m)} \frac{F^{(m)} F^{(m-1)}}{k^{(m)}} + \mathcal{C}_3^{(m)} \frac{\left(F^{(m)}\right)^2}{k^{(m)}} + \mathcal{C}_4^{(m)} \frac{F^{(m)} \epsilon^{(m)}}{k^{(m)}}, \tag{77}$$

where $\mathcal{C}_i^{(m)}$ are coefficients depending on the spectral slice. The tensorial flux $F_{ij}^{(m)}$ is then determined by the scalar flux $F^{(m)}$ assuming the empirical relation

$$F_{ij}^{(m)} = \frac{F^{(m)}}{k^{(m)}} \left[A^{(m)} R_{ij}^{(m)} + \frac{2}{3}(1 - A^{(m)}) k^{(m)} \delta_{ij} \right], \tag{78}$$

where the $A^{(m)}$ coefficients depend also on the wave numbers range. These coefficients are expected to go to unity at small wave numbers and to vanish at high wave numbers where the flow becomes more isotropic. Obviously, the tensorial contraction of $F_{ij}^{(m)}$ in Eq. (78) satisfies the condition $F^{(m)} = \frac{1}{2} F_{ii}^{(m)}$. More information can be found in original papers of Schiestel [5,34,35].

5.3 The dissipative terms

The transport equations of the turbulent stress (45), (48) for one-point statistical models, statistical multiple-scale models require the modeling of the dissipation rate tensor ϵ_{ij}. Due to the fact that the dissipation rate tensor ϵ_{ij} is usually assumed to be quasi-isotropic at high Reynolds number, it is sufficient and more convenient to model the dissipation rate ϵ. The case of homogeneous anisotropic flows is first considered. In full statistical modeling, the dissipation rate represents the spectral flux computed for the splitting wave number $\kappa_1 = \kappa_d$. This characteristic wave number is the inverse of the macroscale related to the dissipation rate and the turbulent kinetic energy by a relation of the type

$$\kappa_1 = \zeta_1 \frac{\epsilon}{k^{3/2}}, \tag{79}$$

where the coefficient ζ_1 is a numerical constant chosen such that κ_1 is located after the inertial range. Inserting the previous relation (79) into Eq. (80)

$$\frac{\partial \kappa_2}{\partial t} = \frac{\mathcal{F}(\kappa_2) - F(\kappa_2)}{E(\kappa_2)}, \tag{80}$$

which is deduced from Eq. (56), and considering also Eq. (46) for evaluating the derivative of the turbulent energy, yields the dissipation rate transport equation

$$\frac{\partial \epsilon}{\partial t} = c_{\epsilon_1} \frac{\epsilon}{k} P - c_{\epsilon_2} \frac{\epsilon^2}{k}, \tag{81}$$

where $c_{\epsilon_1} = 3/2$ and

$$c_{\epsilon_2} = \frac{3}{2} - \frac{k}{\kappa_2 E(\kappa_2)} \left(\frac{\mathcal{F}(\kappa_2)}{\epsilon} - 1 \right). \tag{82}$$

These coefficients c_{ϵ_1} and c_{ϵ_2} are equal to the coefficients commonly used in one point statistical closures. Reference [5] first proposed this alternative derivation of the ϵ equation where the dissipation rate itself is interpreted as a spectral flux rather than a true viscous dissipation. In the case of multiple-scale statistical models, a hierarchy of flux Eq. (77) is solved and the dissipation rate is simply obtained by the flux out of the last spectral range. So, from Eq. (77), in the particular case of two-equation multiscale models

$$\frac{\mathrm{d}F^{(1)}}{\mathrm{d}t} = \mathcal{C}_1^{(1)} \frac{F^{(1)} P^{(1)}}{k^{(1)}} + \mathcal{C}_3^{(1)} \frac{\left(F^{(1)}\right)^2}{k^{(1)}} \tag{83}$$

$$\frac{\mathrm{d}\epsilon}{\mathrm{d}t} = \mathcal{C}_1^{(2)} \frac{\epsilon P^{(2)}}{k^{(2)}} + \mathcal{C}_2^{(2)} \frac{\epsilon F^{(1)}}{k^{(2)}} + \mathcal{C}_3^{(2)} \frac{\epsilon^2}{k^{(2)}}, \tag{84}$$

where $F^{(2)} = \epsilon$, $\epsilon^{(1)} \approx 0$ and $\epsilon^{(2)} \approx 0$.

5.4 The diffusive terms

The diffusion terms which appear in Eq. (48) for the turbulent stresses are modeled assuming a gradient law as usually retained for the statistical model

$$J_{ij}^{(m)} = \frac{\partial}{\partial x_k} \left(\nu \frac{\partial R_{ij}^{(m)}}{\partial x_k} + c_s \frac{k^{(m)}}{\epsilon} R_{kl}^{(m)} \frac{\partial R_{ij}^{(m)}}{\partial x_l} \right), \tag{85}$$

where c_s is a numerical coefficient. In the same approach, the diffusion term of the dissipation rate J_ϵ is also modeled by a general gradient hypothesis

$$J_\epsilon^{(m)} = \frac{\partial}{\partial x_k} \left(\nu \frac{\partial \epsilon}{\partial x_k} + c_\epsilon \frac{k^{(m)}}{\epsilon} R_{kl}^{(m)} \frac{\partial \epsilon}{\partial x_l} \right). \tag{86}$$

6 Transposition to subgrid-scale turbulence models

The approach in the case of large eddy simulations is somewhat different from the one proposed in statistical modeling, but useful transpositions can be made with the previous formalism. In this section, the point of view of the tangent homogeneous space at a point of the non-homogeneous flow field must be still kept in mind. Large eddy simulations make use of filtering operation instead of statistical averaging. It is of interest to remark that definition (2) is indeed a filter operating in Fourier space. As usually made in large eddy simulations, the spectrum is then partitioned using the cutoff wave number $\kappa_1 = \kappa_c$ introduced in the beginning of the inertial range of eddies. In very large eddy simulations, the cutoff may be located before the inertial range. Another wave number $\kappa_2 = \kappa_d$ located at the end of the inertial range of the spectrum can also be used like previously for convenience, assuming that the energy pertaining to higher wavenumbers is entirely negligible. It is then possible to define the large scale fluctuations (resolved scales) $u_i^<$ and the fine scales (modeled scales) $u_i^>$ through the relations

$$u_i^< = \int_{|\boldsymbol{\kappa}| \le \kappa_c} \widehat{u'}_i(\boldsymbol{\kappa}) \exp\left(j \boldsymbol{\kappa} \boldsymbol{\xi}\right) \, \mathrm{d}\boldsymbol{\kappa} \tag{87}$$

$$u_i^> = \int_{|\boldsymbol{\kappa}| \ge \kappa_c} \widehat{u'}_i(\boldsymbol{\kappa}) \exp\left(j \boldsymbol{\kappa} \boldsymbol{\xi}\right) \, \mathrm{d}\boldsymbol{\kappa}. \tag{88}$$

Then, the instantaneous velocity u_i can be decomposed into a statistical part $\langle u_i \rangle$, the large scale fluctuating $u_i^<$ and the small scale fluctuating $u_i^>$ such that $u_i = \langle u_i \rangle + u_i^< + u_i^>$. In the same way, the filtered velocity $\bar{u}_i$ can be computed into its statistical part and its large scale fluctuating such that $\bar{u}_i = \langle u_i \rangle + u_i^<$. The velocity fluctuation u_i' used in the decomposition $u_i = \langle u_i \rangle + u_i'$ contains the large-scale and small-scale fluctuating velocities, $u_i' = u_i^< + u_i^>$. This particular filter, as a spectral truncation, presents some interesting properties

that are not possible with continuous filters. In particular, it can be shown [34,35] that large scale and small scale fluctuations are uncorrelated $\langle \varphi^{>} \psi^{<} \rangle = 0$ implying for instance the relations

$$R_{ij} = \langle u_i u_j \rangle - \langle u_i \rangle \langle u_j \rangle = \langle u_i' u_j' \rangle = \langle u_i^{<} u_j^{<} \rangle + \langle u_i^{>} u_j^{>} \rangle \tag{89}$$

and

$$\langle \bar{u}_i \bar{u}_j \rangle = \langle u_i \rangle \langle u_j \rangle + \langle u_i^{<} u_j^{<}. \rangle \tag{90}$$

In aiming to transpose the statistical models to subgrid-scale models, it is useful to obtain first some interesting relations between the subgrid and statistical stresses that can be deduced from their transport equations in the physical space. Then, we show how the present formalism developed in the spectral space and particularly Eq. (35) is compatible with the usual transport equations of the subgrid-scale tensor in the physical space.

The transport equation of the mean statistical velocity is

$$\frac{\partial \langle u_i \rangle}{\partial t} + \frac{\partial}{\partial x_j} \Big(\langle u_i \rangle \langle u_j \rangle \Big) = -\frac{1}{\rho} \frac{\partial \langle p \rangle}{\partial x_i} + \nu \frac{\partial^2 \langle u_i \rangle}{\partial x_j \partial x_j} - \frac{\partial R_{ij}}{\partial x_j} \tag{91}$$

whereas the transport equation for the filtered Navier–Stokes equations takes the form

$$\frac{\partial \bar{u}_i}{\partial t} + \frac{\partial}{\partial x_j} \left(\bar{u}_i \bar{u}_j \right) = -\frac{1}{\rho} \frac{\partial \bar{p}}{\partial x_i} + \nu \frac{\partial^2 \bar{u}_i}{\partial x_j \partial x_j} - \frac{\partial \tau_(u_i, u_j)}{\partial x_j} \tag{92}$$

in which, following Germano's derivation [51], the subgrid scale tensor which is a function of the velocities u_i and u_j is defined by the relation

$$\tau(u_i, u_j) = \overline{u_i u_j} - \bar{u}_i \bar{u}_j \tag{93}$$

The transport equations for the large scale fluctuation can also be derived easily and we obtain

$$\frac{\partial u_i^{<}}{\partial t} + \frac{\partial}{\partial x_j} \Big(\bar{u}_i \bar{u}_j - \langle u_i \rangle \langle u_j \rangle \Big) = -\frac{1}{\rho} \frac{\partial p^{<}}{\partial x_i} + \nu \frac{\partial^2 u_i^{<}}{\partial x_j \partial x_j} - \frac{\partial}{\partial x_j} \left[\tau(u_i, u_j) - R_{ij} \right] \tag{94}$$

whereas the transport of the small-scale fluctuation is:

$$\frac{\partial u_i^{>}}{\partial t} + \frac{\partial}{\partial x_j} \Big(u_i u_j - \bar{u}_i \bar{u}_j \Big) = -\frac{1}{\rho} \frac{\partial p^{>}}{\partial x_i} + \nu \frac{\partial^2 u_i^{>}}{\partial x_j \partial x_j} + \frac{\partial \tau(u_i, u_j)}{\partial x_j}. \tag{95}$$

Obviously, they add up to give the transport equation of the statistical fluctuating velocity

$$\frac{\partial u_i'}{\partial t} + \frac{\partial}{\partial x_j} \Big(u_i u_j - \langle u_i \rangle \langle u_j \rangle \Big) = -\frac{1}{\rho} \frac{\partial p'}{\partial x_i} + \nu \frac{\partial^2 u_i'}{\partial x_j \partial x_j} + \frac{\partial R_{ij}}{\partial x_j} \tag{96}$$

The work of Germano shows that the form of the transport equations for the subgrid scale tensor remain the same if they are written in terms of central moments, thus showing their generic character. As shown in Ref. [51], the resulting equation is

$$\begin{aligned}
&\frac{\partial \tau(u_i, u_j)}{\partial t} + \frac{\partial}{\partial x_k} \left[\tau(u_i, u_j) \bar{u}_k \right] \\
&= -\frac{\partial \tau(u_i, u_j, u_k)}{\partial x_k} + \nu \frac{\partial^2 \tau(u_i, u_j)}{\partial x_k \partial x_k} \\
&\quad - \frac{1}{\rho} \frac{\partial \tau(p, u_i)}{\partial x_j} - \frac{1}{\rho} \frac{\partial \tau(p, u_j)}{\partial x_i} + \tau \left(p, \frac{\partial u_i}{\partial x_j} + \frac{\partial u_j}{\partial x_i} \right) - 2\nu \, \tau \left(\frac{\partial u_i}{\partial x_k}, \frac{\partial u_j}{\partial x_k} \right) \\
&\quad - \tau(u_i, u_k) \frac{\partial \bar{u}_j}{\partial x_k} - \tau(u_j, u_k) \frac{\partial \bar{u}_i}{\partial x_k}
\end{aligned} \tag{97}$$

with the general definition

$$\tau(f,g) = \overline{fg} - \bar{f}\bar{g} \tag{98}$$

and

$$\tau(f,g,h) = \overline{fgh} - \bar{f}\tau(g,h) - \bar{g}\tau(h,f) - \bar{h}\tau(f,g) - \bar{f}\bar{g}\bar{h} \tag{99}$$

for any turbulent quantities f, g, h. As a result of interest, it can be shown that the function τ verifies the useful following properties

$$\langle \tau(f,g) \rangle = \left\langle f^{>} g^{>} \right\rangle \tag{100}$$

and

$$\langle \tau(f,g,h) \rangle = \left\langle f^{>} g^{>} h^{>} \right\rangle. \tag{101}$$

The transport equation for $\tau(u_i, u_j)$ can also be written in order to single out the role of the statistical mean velocity

$$\begin{aligned}
&\frac{\partial \tau(u_i,u_j)}{\partial t} + \langle u_k \rangle \frac{\partial \tau(u_i,u_j)}{\partial x_k} \\
&= -\frac{\partial}{\partial x_k}\Big[\tau(u_i,u_j,u_k) + \tau(u_i,u_j)u_k^{<}\Big] + \nu \frac{\partial^2 \tau(u_i,u_j)}{\partial x_k \partial x_k} \\
&\quad -\frac{1}{\rho}\frac{\partial \tau(p,u_i)}{\partial x_j} - \frac{1}{\rho}\frac{\partial \tau(p,u_j)}{\partial x_i} + \tau\left(p, \frac{\partial u_i}{\partial x_j} + \frac{\partial u_j}{\partial x_i}\right) - 2\nu\,\tau\left(\frac{\partial u_i}{\partial x_k}, \frac{\partial u_j}{\partial x_k}\right) \\
&\quad -\tau(u_i,u_k)\frac{\partial \langle u_j \rangle}{\partial x_k} - \tau(u_j,u_k)\frac{\partial \langle u_i \rangle}{\partial x_k} - \tau(u_i,u_k)\frac{\partial u_j^{<}}{\partial x_k} - \tau(u_j,u_k)\frac{\partial u_i^{<}}{\partial x_k}.
\end{aligned} \tag{102}$$

The mean Eqs. (58) and (59) pertaining to the wave number ranges $[0, \kappa_1]$, $[\kappa_1, \kappa_2]$ can be recovered by statistical averaging of the Eq. (102) taking into account that $\left\langle \tau_{ij}^{(s)} \right\rangle = R_{ij}^{(2)} = \left\langle u_i^{>} u_j^{>} \right\rangle$ and using the property (100). This equation reads

$$\frac{\partial}{\partial t}\left\langle \tau_{ij}^{(s)} \right\rangle + \langle u_k \rangle \frac{\partial}{\partial x_k}\left\langle \tau_{ij}^{(s)} \right\rangle = P_{ij}^{(2)} + F_{ij}^{(1)} - F_{ij}^{(2)} + \Psi_{ij}^{(2)} + J_{ij}^{(2)}, \tag{103}$$

where

$$P_{ij}^{(2)} = -\left\langle \tau_{ik}^{(s)} \right\rangle \frac{\partial \langle u_j \rangle}{\partial x_k} - \left\langle \tau_{jk}^{(s)} \right\rangle \frac{\partial \langle u_i \rangle}{\partial x_k}, \tag{104}$$

$$F_{ij}^{(1)} = -\left\langle \tau_{ik}^{(s)} \frac{\partial u_j^{<}}{\partial x_k} \right\rangle - \left\langle \tau_{jk}^{(s)} \frac{\partial u_i^{<}}{\partial x_k} \right\rangle, \tag{105}$$

$$F_{ij}^{(2)} = 2\nu \left\langle \frac{\partial u_i^{>}}{\partial x_k} \frac{\partial u_j^{>}}{\partial x_k} \right\rangle \approx \epsilon_{ij}, \tag{106}$$

$$\Psi_{ij}^{(2)} = \left\langle p^{>} \left(\frac{\partial u_i^{>}}{\partial x_j} + \frac{\partial u_j^{>}}{\partial x_i} \right) \right\rangle, \tag{107}$$

$$\begin{aligned}
J_{ij}^{(2)} &= -\frac{\partial}{\partial x_k}\Big[\left\langle u_i^{>} u_j^{>} u_k^{>} \right\rangle + \left\langle \tau(u_i,u_j)u_k^{<} \right\rangle\Big] \\
&\quad -\frac{1}{\rho}\frac{\partial}{\partial x_j}\left\langle p^{>} u_i^{>} \right\rangle - \frac{1}{\rho}\frac{\partial}{\partial x_i}\left\langle p^{>} u_j^{>} \right\rangle + \nu \frac{\partial^2}{\partial x_k \partial x_k}\left\langle \tau_{ij}^{(s)} \right\rangle.
\end{aligned} \tag{108}$$

Similarly, the resolved scale tensor can be defined by the relation

$$\tau^{(r)}(u_i,u_j) = \bar{u}_i \bar{u}_j - \langle u_i \rangle \langle u_j \rangle \tag{109}$$

with the property $\left\langle \tau^{(r)}(u_i,u_j)\right\rangle = \left\langle u_i^< u_j^<\right\rangle$. So that, one can remark that the Reynolds stress tensor R_{ij} can be computed by the sum of the statistical average of subgrid and resolved stresses $R_{ij} = \left\langle \tau^{(s)}(u_i,u_j)\right\rangle + \left\langle \tau^{(r)}(u_i,u_j)\right\rangle$. It is also possible then to determine the transport equation of averaged resolved stress $\left\langle \tau_{ij}^{(r)}\right\rangle = R_{ij}^{(1)} = \left\langle u_i^< u_j^<\right\rangle$, and we obtain

$$\frac{\partial}{\partial t}\left\langle \tau_{ij}^{(r)}\right\rangle + \langle u_k\rangle \frac{\partial}{\partial x_k}\left\langle \tau_{ij}^{(r)}\right\rangle = P_{ij}^{(1)} - F_{ij}^{(1)} + \Psi_{ij}^{(1)} + J_{ij}^{(1)} - \epsilon_{ij}^{(1)} \tag{110}$$

where

$$P_{ij}^{(1)} = -\left\langle \tau_{ik}^{(r)}\right\rangle \frac{\partial \left\langle u_j\right\rangle}{\partial x_k} - \left\langle \tau_{jk}^{(r)}\right\rangle \frac{\partial \langle u_i\rangle}{\partial x_k}, \tag{111}$$

$$F_{ij}^{(1)} = -\left\langle \tau_{ik}^{(s)} \frac{\partial u_j^<}{\partial x_k}\right\rangle - \left\langle \tau_{jk}^{(s)} \frac{\partial u_i^<}{\partial x_k}\right\rangle, \tag{112}$$

$$\Psi_{ij}^{(1)} = \left\langle p^< \left(\frac{\partial u_i^<}{\partial x_j} + \frac{\partial u_j^<}{\partial x_i}\right)\right\rangle, \tag{113}$$

$$\begin{aligned} J_{ij}^{(1)} = &-\frac{\partial}{\partial x_k}\left[\left\langle u_i^< u_j^< u_k^<\right\rangle - \left\langle \tau(u_i,u_j)u_k^<\right\rangle\right] \\ &-\frac{1}{\rho}\frac{\partial}{\partial x_j}\left\langle p^< u_i^<\right\rangle - \frac{1}{\rho}\frac{\partial}{\partial x_i}\left\langle p^< u_j^<\right\rangle + \nu \frac{\partial^2}{\partial x_k \partial x_k}\left\langle \tau_{ij}^{(r)}\right\rangle, \end{aligned} \tag{114}$$

$$\epsilon_{ij}^{(1)} = 2\nu \left\langle \frac{\partial u_i^<}{\partial x_k}\frac{\partial u_j^<}{\partial x_k}\right\rangle \ll F_{ij}^{(2)}. \tag{115}$$

As previously mentioned, the mathematical formalism put in place in Sect. 4.3 allows one to recover formally Eq. (103) as well as Eq. (110) which are now deduced from the spectral space. In particular, Eq. (103) is formally identical to Eq. (59)

$$\frac{\mathrm{D}R_{ij}^{(2)}}{\mathrm{D}t} = P_{ij}^{(2)} + F_{ij}^{(1)} + \Psi_{ij}^{(2)} + J_{ij}^{(2)} - \epsilon_{ij} \tag{116}$$

with the definitions

$$P_{ij}^{(2)} = \int_{\kappa_1}^{\kappa_2} \mathcal{P}_{ij}(\boldsymbol{X},\kappa)\mathrm{d}\kappa = -R_{ik}^{(2)}\frac{\partial \left\langle u_j\right\rangle}{\partial x_k} - R_{jk}^{(2)}\frac{\partial \langle u_i\rangle}{\partial x_k}, \tag{117}$$

$$F_{ij}^{(1)} = \mathcal{F}_{ij}^{(1)} - \varphi_{ij}(\boldsymbol{X},\kappa)\frac{\partial \kappa_1}{\partial t}, \tag{118}$$

$$\mathcal{F}_{ij}^{(1)} = -\int_0^{\kappa_1} \mathcal{T}_{ij}(\boldsymbol{X},\kappa)\mathrm{d}\kappa, \tag{119}$$

$$\Psi_{ij}^{(2)} = \int_{\kappa_1}^{\kappa_2} \Pi_{ij}(\boldsymbol{X},\kappa)\mathrm{d}\kappa, \tag{120}$$

$$J_{ij}^{(2)} = \int_{\kappa_1}^{\kappa_2} \mathcal{J}_{ij}(\boldsymbol{X},\kappa)\mathrm{d}\kappa, \tag{121}$$

where $\epsilon_{ij} \approx F_{ij}^{(2)}$. In contrast to multiple-scale models which require the modeling of the transfer terms F_{ij} in order to close the system equation, the term $F_{ij}^{(1)}$, which appears in Eq. (116), is directly computed when

performing large eddy simulations. Indeed, using the relation

$$R_{ik}^{(2)} \frac{\partial \langle u_i \rangle}{\partial x_k} = \left\langle \tau_{ik}^{(s)} \frac{\partial \langle u_i \rangle}{\partial x_k} \right\rangle \tag{122}$$

and introducing the large-scale fluctuating velocity component, the production term in Eq. (117) can be decomposed in the following way:

$$P_{ij}^{(2)} = -\left\langle \tau_{ik}^{(s)} \frac{\partial \bar{u}_j}{\partial x_k} \right\rangle - \left\langle \tau_{jk}^{(s)} \frac{\partial \bar{u}_i}{\partial x_k} \right\rangle + \left\langle \tau_{ik}^{(s)} \frac{\partial u_j^<}{\partial x_k} \right\rangle + \left\langle \tau_{jk}^{(s)} \frac{\partial u_i^<}{\partial x_k} \right\rangle \tag{123}$$

showing that

$$P_{ij}^{(2)} + F_{ij}^{(1)} = -\left\langle \tau_{ik}^{(s)} \frac{\partial \bar{u}_j}{\partial x_k} \right\rangle - \left\langle \tau_{jk}^{(s)} \frac{\partial \bar{u}_i}{\partial x_k} \right\rangle, \tag{124}$$

where $F_{ij}^{(1)}$ in Eq. (124) is given by Eq. (105). Equation (105) shows that the spectral flux $F_{ij}^{(1)}$ at the cutoff wave number corresponds to the transfer process due to the action of large-scale structures on the subgrid-scale turbulence. Taking into account Eq. (124), the transport Eq. (116) of the subgrid turbulent stresses can be finally rewritten in the usual form

$$\frac{\partial}{\partial t} \left\langle \tau_{ij}^{(s)} \right\rangle + \langle u_k \rangle \frac{\partial}{\partial x_k} \left\langle \tau_{ij}^{(s)} \right\rangle = -\left\langle \tau_{ik}^{(s)} \frac{\partial \bar{u}_j}{\partial x_k} \right\rangle - \left\langle \tau_{jk}^{(s)} \frac{\partial \bar{u}_i}{\partial x_k} \right\rangle + \Psi_{ij}^{(2)} + J_{ij}^{(2)} - \epsilon_{ij}, \tag{125}$$

whereas equation of the subfilter energy is then obtained by tensor contraction of Eq. (125)

$$\frac{\partial}{\partial t} \left\langle k^{(s)} \right\rangle + \langle u_k \rangle \frac{\partial}{\partial x_k} \left\langle k^{(s)} \right\rangle = -\left\langle \tau_{ij}^{(s)} \frac{\partial \bar{u}_i}{\partial x_j} \right\rangle + J^{(2)} - \epsilon \tag{126}$$

For LES, Eqs. (97) will be solved in space and time. These equations are fluctuating and have a similar form as Eqs. (125) and (126). In this case, the convective term in Eq. (125) involves the filtered velocity instead of the mean statistical velocity. A part of this term $\partial\left(u_k^< \tau_{ij}^{(s)}\right)/\partial x_k$ is thus reported in turbulent diffusion terms. These fluctuating equations read

$$\frac{\partial \tau_{ij}^{(s)}}{\partial t} + \bar{u}_k \frac{\partial \tau_{ij}^{(s)}}{\partial x_k} = P_{ij}^{(s)} + \Psi_{ij}^{(s),(2)} + J_{ij}^{(s),(2)} - \epsilon_{ij}^{(s)}, \tag{127}$$

where the (s) values denotes fluctuating instantaneous quantities and $P_{ij}^{(s)}$ is the production term defined by

$$P_{ij}^{(s)} = -\tau_{ik}^{(s)} \frac{\partial \bar{u}_j}{\partial x_k} - \tau_{jk}^{(s)} \frac{\partial \bar{u}_i}{\partial x_k}. \tag{128}$$

The corresponding equation for subfilter energy reads

$$\frac{\partial k^{(s)}}{\partial t} + \bar{u}_k \frac{\partial k^{(s)}}{\partial x_k} = P^{(s)} + J^{(s),(2)} - \epsilon^{(s)}, \tag{129}$$

where $P^{(s)} = P_{mm}^{(s)}/2$. Because of the properties in the Fourier space of the truncation filter, it appears that the mean statistical and filtered equations can both be written in a similar form. As a consequence, we shall assume that closures approximations used for the statistical partially averaged equations also prevail in the case of large eddy numerical simulations. It is of interest to note that the present formalism is in fact the essence of the partially integrated transport model (PITM), first developed by Schiestel and Dejoan [16] for the transport Eq. (129) of the subgrid-scale turbulent energy $k^{(s)} = \frac{1}{2}\tau_{mm}^{(s)}$ and by Chaouat and Schiestel [17] for the transport Eq. (127) of the subgrid-scale turbulent stress tensor $\tau_{ij}^{(s)}$. In the subfilter models, the redistribution term $\Psi_{ij}^{(s),(2)}$ which appears in Eq. (127) is also decomposed into a slow and a rapid part, $\Psi_{ij}^{(s),(2,1)}$ and $\Psi_{ij}^{(s),(2,2)}$ in the subgrid-scale range. The slow term is modeled by a twofold hypothesis. It first assumes that usual statistical Reynolds stress models must be recovered in the limit where the cutoff wave number κ_1 goes to zero and also

that the return to isotropy is increased at higher wave numbers [17], as adopted in multiple-scale models. So that we obtain the modeled terms as

$$\Psi_{ij}^{(s),(2,1)} = -c_1^{(s)} \frac{\epsilon^{(s)}}{k^{(s)}} \left(\tau_{ij}^{(s)} - \frac{1}{3} \tau_{mm}^{(s)} \delta_{ij} \right) \tag{130}$$

and

$$\Psi_{ij}^{(s),(2,2)} = -c_2^{(s)} \left(P_{ij}^{(s)} - \frac{2}{3} P_{mm}^{(s)} \delta_{ij} \right) \tag{131}$$

and $c_1^{(s)}$ is now a continuous function of the cutoff wave number κ_1 that defines the filter width. The value of this coefficient has to be calibrated by reference to experiments (see for instance application of partially integrated transport models in the remainder of the present paper). For LES or hybrid RANS/LES approaches, the transport equation of the dissipation rate used in subfilter models is somewhat different from Eq. (81). Considering the cutoff wave number $\kappa_1 = \kappa_c$ given by the filter width, the splitting wave number κ_2 is then determined by the dimensional relation

$$\kappa_2 - \kappa_1 = \zeta_1 \frac{\epsilon}{\left\langle k^{(s)3/2} \right\rangle}, \tag{132}$$

where ζ_1 is a coefficient which may be depended on the spectrum shape and on the Reynolds number. Note that this relation is simply an application of Eq. (76) for a particular splitting decomposition of the spectrum. The dissipation rate equation is then an adaptation of Eq. (80). Taking into account Eq. (80) one can easily obtain

$$\frac{\partial \epsilon^{(s)}}{\partial t} = c_{\epsilon_1}^{(s)} \frac{\epsilon}{k^{(s)}} P^{(s)} - c_{\epsilon_2}^{(s)} \frac{\left(\epsilon^{(s)}\right)^2}{k^{(s)}}, \tag{133}$$

where $c_{\epsilon_1}^{(s)} = 3/2$ and

$$c_{\epsilon_2}^{(s)} = \frac{3}{2} - \frac{\left\langle k^{(s)} \right\rangle}{\kappa_2 E(\kappa_2)} \left(\frac{\mathcal{F}(\kappa_2)}{\epsilon} - 1 \right), \tag{134}$$

setting $\kappa_2 \gg \kappa_1$, and $E(\kappa_2) \ll E(\kappa_1)$. Eqs. (82) and (134) show that the coefficients $c_{\epsilon_2}^{(s)}$ and c_{ϵ_2} are functions of the spectrum shape. We emphasize that if the usual ϵ Eq. (81) and Eq. (133) derived from reasoning in the subgrid range are formally different, it appears, however, that the statistical average of $\epsilon^{(s)}$ is the usual dissipation rate, $\left\langle \epsilon^{(s)} \right\rangle = \epsilon$. We remark also that we have used a reasoning based on statistical spectra, like in multiple scale models, considering that the dissipation rate equation is largely intuitive in its derivation. In practice, comparison of Eq. (82) and (134) provides a more convenient form of the coefficient $c_{\epsilon_2}^{(s)}$ such as ([16]):

$$c_{\epsilon_2}^{(s)} = c_{\epsilon_1} + \frac{\left\langle k^{(s)} \right\rangle}{k} \left(c_{\epsilon_2} - c_{\epsilon_1} \right). \tag{135}$$

The function $k^{(s)}/k$, which appears in Eq. (135), is then calibrated in an equilibrium situation by referring to a universal spectrum distribution compatible with the Kolmogorov law in the inertial wave number range in nearly equilibrium flows. Practical formulations can be devised in the form

$$c_{\epsilon_2}^{(s)} = c_{\epsilon_2}^{(s)}(\eta), \tag{136}$$

where $\eta = \kappa_1 k^{3/2}/\epsilon$ with the limiting behavior

$$\frac{\left\langle k^{(s)} \right\rangle}{k} = \frac{3}{2} C_K \eta^{-\frac{2}{3}} \tag{137}$$

at large wave numbers where C_K is the Kolmogorov constant. This behavior is in agreement with the work of Rubinstein and Zhou [52,53], who derived the ϵ equation from analytical models and exploring also the limits of the standard ϵ equation when high unsteadiness is imposed [54]. For non-homogenous flows, the diffusion term J_ϵ is also embedded into Eqs. (81) and (133).

With the tangent homogeneous space in mind, let us remark finally that when very large filter widths are used, the filter width has to be dissociated from the grid itself, because the grid must always be fine enough to capture the mean flow non-homogeneities.

7 Application of multiple-scale RANS models

7.1 Two and three-scale stress model $R_{ij} - F$

For usual applications, the two-scale models are developed considering two splitting wave numbers [5,45]. In that case, the numerical system to be solved is composed of the transport equations of the partial Reynolds stresses $R_{ij}^{(1)}$, $R_{ij}^{(2)}$, the partial turbulent kinetic energies $k^{(1)}$, $k^{(2)}$, and the spectral fluxes $F^{(1)}$, $F^{(2)}$ where $F^{(2)} = \epsilon$. The coefficients $c_1^{(m)}$ and $c_2^{(m)}$ are calibrated on homogeneous flows using direct numerical simulations [55] that determine the spectral behavior of the pressure-strain correlations. In practice, the numerical constants retained are $c_1^{(1)} = 1.20, c_1^{(2)} = 4.00, c_2^{(m)} = 0.5$ $(m = 1, 2)$. Three scale-models are also considered as an extension of two-scale models. The numerical system is then composed of the variable set $R_{ij}^{(1)}$, $R_{ij}^{(2)}$, $R_{ij}^{(3)}$, $k^{(1)}$, $k^{(2)}$, $k^{(3)}$, $F^{(1)}$, $F^{(2)}$, $F^{(3)}$ where $F^{(3)} = \epsilon$. In this case the numerical constants are $c_1^{(1)} = 1.05$, $c_1^{(2)} = 1.80$, $c_1^{(3)} = 8.00$, $c_2^{(m)} = 0.5$ $(m = 1, 2, 3)$. More advanced multiple-scale models are straightforward to settle following the mathematical formalism already developed. Note that the scope of applications of multiple-scale models is mainly devoted to turbulent flows that are out of equilibrium.

7.2 Axisymmetric contraction

This is a typical example. The experiment on the axisymmetric contraction of grid turbulence worked out by Uberoi and Wallis [56] has been considered for analyzing the two-scale model [5] in its capabilities to predict flows which present non-equilibrium spectra. In this experiment, initial fluid particles that are convected into a channel are subjected to a sudden contraction. Both experimental and numerical evolutions of the ratio $\langle u_1'^2 \rangle / \langle u_2'^2 \rangle$ in the axisymmetric contraction duct are described in Fig. 1. From the measurements, it can be seen that the ratio $\langle u_1'^2 \rangle / \langle u_2'^2 \rangle$ produced by the grid is of order 1.4 and returns to unity through the contraction. Somewhat surprisingly, the ratio monotonically continues increasing in the downstream straight duct section to its pre-contraction value. This is an interesting paradox, which can be explained if working in the spectral space. In the initial flow located upstream the contraction, it can be assumed that the anisotropy is mainly concentrated in the large scales of motions. As expected, the axisymmetric contraction reduces the flow anisotropy because of the rapid deformation due to the mean flow and produces quasi identical normal stresses. But one should keep in mind that the spectral sharing out between the small and large scale is different for each normal stress component and anisotropy still remains at the spectral level (large scale and small scale anisotropies are just compensating). When passing after the contraction to a straight section, the small scale motions return more rapidly to isotropy than the large scales. So this phenomena reveals in fact the anisotropy of the large scale that was temporarily hidden by the small scales before the contraction. As a result of interest, Schiestel's computation [5] indicates that the two-scale model succeeds in reproducing this paradoxical phenomenon, which consists of a "return to anisotropy", contrary to single-scale models which cannot reproduce this behavior. Even more advanced single-scale models cannot reproduce this behavior because they always state that Ψ_{ij} goes to zero when the anisotropy tensor vanishes $a_{ij} = 0$. The simple reason being that an isotropic Reynolds stress tensor does not mean isotropic turbulence, the anisotropy may be distributed among spectral wavenumbers. Indeed, one-scale modeling using the Rotta's hypothesis or higher order approximations cannot account for spectral information, and consequently cannot spontaneously "return to anisotropy", from an isotropy state of the Reynolds stresses. This dual feature of relaxation of the large scales and the small scales was recognized by Lee and Reynolds [57] in their numerical simulations of homogeneous turbulence from irrotational strains. They indeed found overshoot phenomena that the authors explained qualitatively by the fact that in the initial period of relaxation, the small scales relax rapidly, while the large scale anisotropy overshoots or relaxes at a slow rate, depending on the strain history of the initial field.

7.3 Decay of isotropic turbulence with perturbed initial spectrum

The decay of isotropic turbulence is often studied for analyzing the performances of turbulence models or calibrating numerical coefficients. Usually, nearly equilibrium distribution are considered. The measurements of Comte-Bellot and Corrsin [58] are generally chosen as an experimental reference. In the initial region of

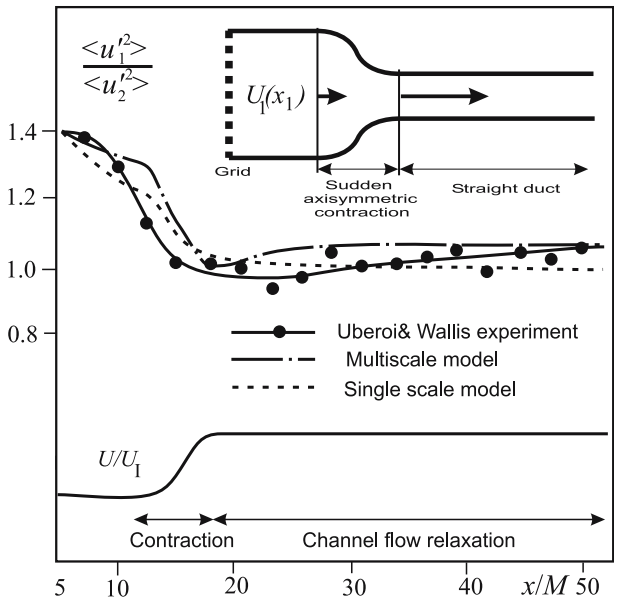

Fig. 1 Evolution of the ratio $\langle u_1'^2 \rangle / \langle u_2'^2 \rangle$ in the Uberoi and Wallis experiment [56] compared to numerical prediction [5]

decay, the turbulence energy is found to verify a power law $k/k_0 = t^{-n}$ with n=1.28. In the present case, we consider an initial spectrum which is artificially perturbed by modification of energy levels departing from usual equilibrium spectra. The aim is to study the influence of initial spectral distribution on the decay law as an illustration of out of spectral equilibrium situations. Figure 2 describes the evolutions of the the ratio $\langle u_1'^2 \rangle / \langle u_2'^2 \rangle$ versus time (the quantity U denotes the mean convective velocity and M is the mesh size in the experiment) for an unperturbed initial spectrum denoted B and two perturbed initial spectra denoted A and C. The spectra are modified, respectively, by decreasing the large scale energy (A) or increasing the large scale energy (C). For the unperturbed spectrum, the decay law given by the standard $k - \epsilon$ model according the relation $k/k_0 = t^{\frac{1}{1-c_{\epsilon_2}}}$ that leads the slope of decay close to n=1.11 if considering the usual value $c_{\epsilon_2} = 1.90$. This value obtained from a consensus on several experiments is somewhat lower than Comte-Bellot's value, but has no consequence for the present purpose. The computation performed with the two-scale stress model [59] indicates that a peak in large scale energy (resp. a defect in large scale energy) implies a decrease (resp. an increase) of the decay rate of turbulence. These results are found to be in qualitative agreement with EDQNM spectral models predictions by Cambon et al. [21]. As for the previous test case, this turbulence spectral effect due to departure from equilibrium cannot be reproduced using single-scale turbulence models.

8 Application of partially integrated transport models (PITM) for LES and hybrid models

8.1 Pulsed turbulent channel flow

A partially integrated transport model based on Eq. (129) for the subfilter turbulent kinetic energy and Eq. (133) for the dissipation rate has been developed by Schiestel and Dejoan [16] for LES simulations of unsteady flows on coarse grids which present non-equilibrium turbulence spectrum. When coarse grids are used, the cutoff wave number can be located before the inertial zone and the modeled part of the spectrum includes non-universal energetic eddies. In this new formulation, the characteristic length scale of subfilter turbulence is not given by the spatial mesh discretization step size but is computed by the dissipation rate equation. This method enables one to bridge RANS models and LES methods in a continuous way without interface as in usual zonal hybrid models. The formalism is compatible with the two extreme limits that are, on one hand, the DNS and, on the other hand, the statistical $k - \epsilon$ model of Launder and Sharma [60]. The channel flow subjected to a periodic forcing produced by a superimposed sinusoidal longitudinal mean pressure gradient like in the experiment of Binder and Kunéy [61], Tardu and Binder [62] has been considered for illustrating the potentials of the model. Depending of the imposed frequency of oscillations of the mean pressure gradient in the channel,

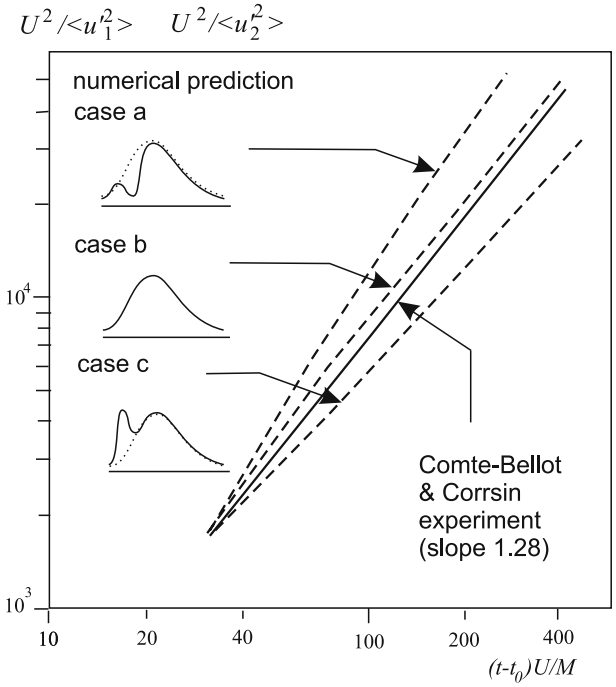

Fig. 2 Isotropic decay of the turbulent kinetic energy in the Comte-Bellot and Corrsin experiment [58] compared to numerical prediction [59]

the experimental results have exhibited strong lag effects between the modulation of the turbulent stress and the forcing. LES simulation has been performed on relatively coarse grid ($32 \times 64 \times 62$) in the streamwise, spanwise and normal directions to the wall, respectively. As shown in the original paper by Schiestel and Dejoan [16], the main result of interest is that the time delay of the turbulent intensity relative to the forcing was much better predicted by the two-equation PITM model than by the Smagorinsky model.

8.2 Injection induced turbulent channel flows

In the framework of PITM models, Chaouat and Schiestel [17,18] have developed a more advanced subgrid-model based on transport Eq. (127) for the subfilter stresses and Eq. (133) for the dissipation rate. This model embodies the same basic concepts as the two equation subfilter model [16] but takes into account all the transport equations of the stress components $R_{ij}^{(s)}$. This allows a more realistic description of the flow anisotropy than eddy viscosity models and takes into account more precisely the turbulent processes of production, transfer, pressure redistribution effects and dissipation. Moreover, some backscatter effects can possibly arise. Like the companion two equation model, the present model has been developed in order to remain consistent when the cutoff is varied between the two extreme limits corresponding on one side of the spectrum to full statistical RSM model of Launder and Shima [63] and on the other side to DNS (the model becomes useless in this case). This modeling strategy is motivated by the idea that the recognized advantages of usual second order closures (RSM) [7,8] are worth making transposition into subgrid-scale modeling when the SGS part is not small compared to the resolved part. The application to the channel flow with wall mass injection which undergoes the development of natural unsteadiness with a transition process from laminar to turbulent regime is considered for illustrating the potentials of the model. This case is of central interest for engineering applications in solid rocket motors (SRM) as mentioned by instance by Gany and Aharon [64] or Chaouat and Schiestel [65]. Figure 3 shows the schematic of channel flow with fluid injection. The dimensions of the length, height and width channel are respectively 58.1, 2.06 and 1.03 cm. The present large eddy simulation has been performed on a medium grid ($400 \times 44 \times 80$) in the streamwise, spanwise and normal directions to the wall. Note that a more conventional approach using detached eddy simulation (DES) commonly applied in engineering applications or the dynamic model [66] requires a more refined grid for computing accurately this type of flow [67]. In particular, a strong decrease in the number of grid points has been obtained (64 %) in regard with the LES

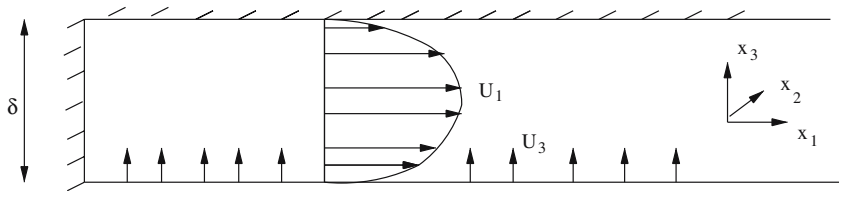

Fig. 3 Schematic of channel flow with fluid injection of Vecla setup

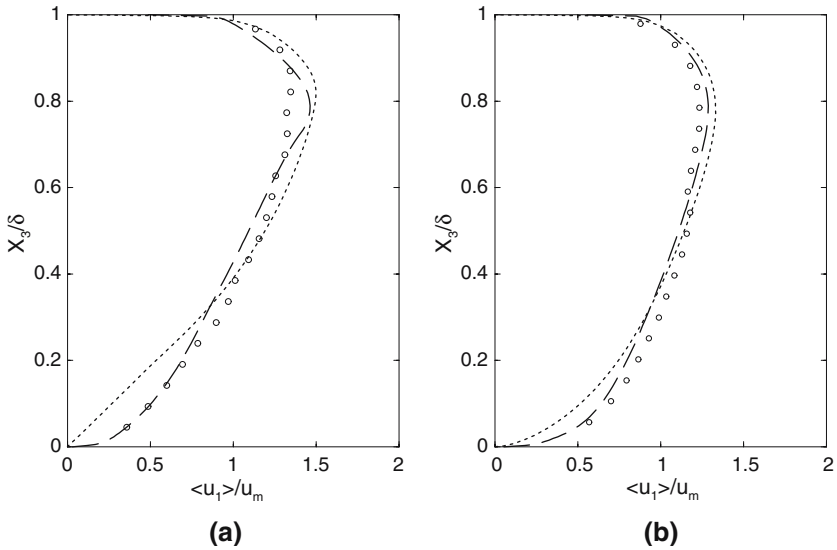

Fig. 4 Mean velocity profiles normalized by the bulk velocity $\langle u_1 \rangle / u_m$ in different cross sections **a** $x_1 = 22$ cm; **b** 57 cm; *dotted line* RSM computations [69]; *dashed line* LES simulation [17]; *circle* experimental data [70]

simulation of Apte and Yang [68] for an almost similar computational domain, because of the present PITM model that is well suited for simulating flows on coarse grids. In this study, the viscosity and turbulent stress profiles produced by the present LES simulation [17] as well as the RANS computation using a variant RSM model of Launder and Shima [63,69] have been compared with the experimental data worked out by Avalon et al. [70] that describes injection induced flow in the specific setup at ONERA. Figure 4 shows the velocity profiles $\langle u_1 \rangle / u_m$ normalized by the bulk velocity u_m in two locations of the channel at $x_1 = 22$ cm and 57 cm where the flow regimes are, respectively, laminar and then turbulent. It appears that the RMS computation as well as the LES simulation produce velocity profiles that agree rather well with the experimental data. Figure 5 describes the streamwise turbulent stresses $\left\langle u_1' u_1' \right\rangle / u_m$ in different stations of the channel at $x_1 =$ 40 cm, 45, 50 and 57 cm. As a result of interest, one can observe that both the RSM computation and the LES simulation reasonably well predict the turbulence intensity of the flow in the downstream transition location where the flow presents a turbulent regime, except, however, in the immediate vicinity of the wall region. Differences between the RSM and LES stress results should probably due to the triggering of the transition which not occurs in the same location of the channel. Therefore, it appears that the mean flow variables such that the velocities and stresses can be accurately computed both by RANS and LES approaches although the turbulence modeling is quite different. But contrary to full statistical modeling, only LES simulation is able to provide the structural information of the flow. Figure 6 shows the isosurfaces of the instantaneous spanwise filtered vorticity $\bar{\omega}_2 = \partial \bar{u}_3 / \partial x_1 - \partial \bar{u}_1 / \partial x_3$ in the channel and reveals the detail of the flow structures subjected to mass injection. In the first part of the channel where the flow is laminar, the isosurfaces form a parallel plane up to the injection surface. Then, the isosurfaces show the presence of roll-up vortex structures in the spanwise direction indicating the transitional and turbulent flow regime. Moreover, because of the injection, the three-dimensional structures are squeezed upward in the normal direction to the axial flow. In spite of the coarse grid computation, it is remarkable that the present LES calculation succeeded in obtaining a good qualitative prediction of these structures that are quite similar to those simulated by Apte and Yang [68].

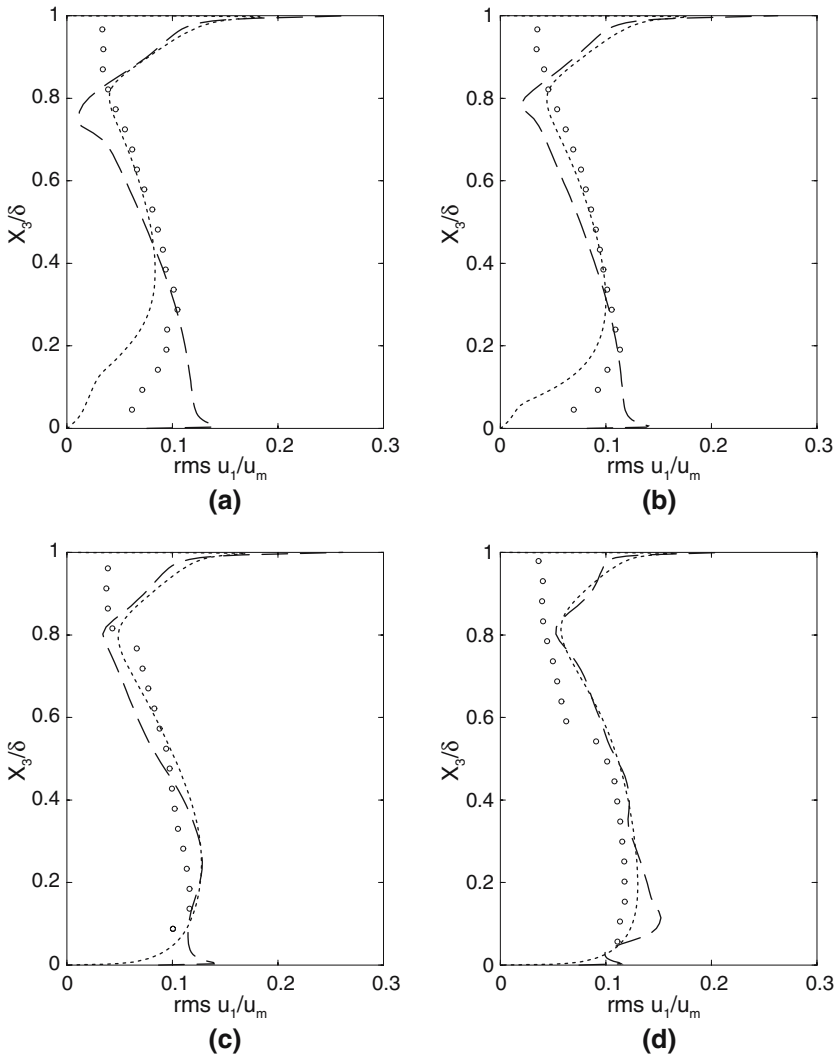

Fig. 5 Streamwise turbulent stresses $\langle u_1' u_1' \rangle^{1/2} / u_m$ in different cross sections **a** $x_1 = 40$ cm; **b** 45 cm; **c** 50 cm; **d** 57 cm. *dotted line* RSM computations [69]; *dashed line* LES simulation [17]; *circle* experimental data [70]

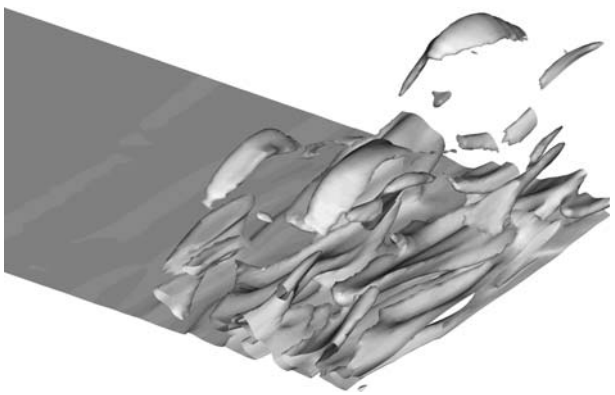

Fig. 6 Isosurfaces of instantaneous filtered vorticity vector $\bar{\omega}_i = \epsilon_{ijk} \partial \bar{u}_k / \partial x_j$ in the spanwise direction $|\bar{\omega}_2| = 3000$ (1/s). LES simulation [17]. Experimental cold flow setup of Avalon [70]

9 Conclusion

While many modeling approaches have been developed often independently up to now, a theoretical formalism that allows transposition of turbulence modeling closures from RANS to LES has been presented. We show that a full or partial integration over the wave numbers of the dynamic equation of the spectral velocity correlation tensor allows one to recover respectively usual one-point statistical closures, statistical multiple-scale models as well as subfilter transport models used for LES (using PITM). The proposed approach makes use of the concept of tangent homogeneous field, considered as deriving from the first term in the Taylor development of local mean velocity field. Higher order approximations bring much complexities and have not been considered here. The use of the statistical filter leads to a three term decomposition of the turbulence field introducing a mean value, a large scale fluctuation and a fine grained fluctuation. The equations obtained for statistical multiple scale transport models are exact for homogeneous anisotropic turbulence and when the filter width goes to infinity ($\Delta \to \infty$, $\kappa_c \to 0$ and $\overline{U} \to \langle U \rangle$), the filtered field goes to the statistical mean field. This property is lost in non-homogeneous fields, but it can be preserved, at least formally, if the concept of homogeneous tangent space is used. In the case of LES, the same statistical filter can be used to derive transport equation that have the same form as in statistical multiscale. For LES of non-homogeneous flows, an approximate approach consists of supplementing additional diffusion terms to the homogeneous model. In the homogeneous case, the formalism for multiple scale statistical models and the PITM formalism will coincide. Modeling of the pressure-strain correlation, transfer, dissipation and diffusion terms for each type of model have been also presented and discussed by reference to physical behaviors. In particular, emphasis has been put on the transfer and dissipative terms that can be indeed interpreted as spectral fluxes. Then, typical experiments that describe flow situations with significant non-equilibrium spectrum have been considered for illustrating some potentials of these models. The main insight of the present formalism developed in the spectral space is therefore to bridge URANS models and LES simulations from a theoretical point of view showing a promising route of new future developments in hybrid models with seamless coupling that can be done in this framework.

A Appendix: Analytical integration for spectral tensor terms

Integration of the different terms defined in paragraph 4.1 can be performed using the reciprocal change in variables. Indeed, considering the vector difference $\xi_m = x_{mB} - x_{mA}$ and the midway position $X_m = \frac{1}{2}(x_{mA} + x_{mB})$, the reciprocal variables are then defined as $x_{mA} = X_m - \frac{1}{2}\xi_m$ and $x_{mB} = X_m + \frac{1}{2}\xi_m$. Full integrations in the spectral space of the quantities Π_{ij}, $\mathcal{E}_{ij}$ and $\mathcal{J}_{ij}$ that appear in Eq. (35) require the calculation of first and second spatial derivatives, with respect to the distance ξ_m as well as the limiting condition when ξ_m goes to zero. Using the above change of variables, we see that it is a straightforward matter to show that the first and second derivatives are expressed in the following way

$$\frac{\partial}{\partial \xi_m} = \frac{1}{2}\left(\frac{\partial}{\partial x_{mB}} - \frac{\partial}{\partial x_{mA}}\right), \tag{138}$$

and

$$\frac{\partial^2}{\partial \xi_m \partial \xi_m} = \frac{1}{4}\left(\frac{\partial^2}{\partial x_{mA}\partial x_{mA}} - 2\frac{\partial^2}{\partial x_{mA}\partial x_{mB}} + \frac{\partial^2}{\partial x_{mB}\partial x_{mB}}\right). \tag{139}$$

When applying relation (139) for the turbulent Reynolds stress $\tau_{ij} = \left\langle u'_{iA} u'_{jB} \right\rangle (x_{mA}, x_{mB})$, one has to keep in mind that the fluctuation u'_{jB} is treated as a function of x_{mB} only. This procedure allows the computation of the first derivative $\partial \left\langle u'_{iA} u'_{jB} \right\rangle / \partial \xi$ as well as the second derivative $\partial^2 \left\langle u'_{iA} u'_{jB} \right\rangle / \partial \xi^2$. Thus, we obtain

$$\left[\frac{\partial \left\langle u'_{iA} u'_{jB} \right\rangle}{\partial \xi_m}\right]_{\xi_m = 0} = \frac{1}{2}\left[\left\langle u'_i \frac{\partial u'_j}{\partial x_m} \right\rangle - \left\langle u'_j \frac{\partial u'_i}{\partial x_m} \right\rangle\right], \tag{140}$$

$$\left[\frac{\partial^2 \left\langle u'_{iA} u'_{jB} \right\rangle}{\partial \xi_m \partial \xi_m}\right]_{\xi_m = 0} = \frac{1}{4}\frac{\partial^2 \left\langle u'_i u'_j \right\rangle}{\partial x_m \partial x_m} - \left\langle \frac{\partial u'_i}{\partial x_m} \frac{\partial u'_j}{\partial x_m} \right\rangle \tag{141}$$

with $x_m = x_{mA} = x_{mB}$ and

$$\frac{\partial u'_{iA}}{\partial x_{mA}} = \frac{\partial u'_{iB}}{\partial x_{mB}} = \frac{\partial u'_i}{\partial x_m}. \tag{142}$$

The first derivative $\partial/\partial X_m$ is computed by

$$\frac{\partial}{\partial X_m} = \left(\frac{\partial}{\partial x_{mA}} + \frac{\partial}{\partial x_{mB}}\right), \tag{143}$$

that implies in particular

$$\left[\frac{\partial \left\langle u'_{iA} u'_{jB}\right\rangle}{\partial X_m}\right]_{\xi=0} = \frac{\partial \left\langle u'_i u'_j\right\rangle}{\partial x_m} \tag{144}$$

and

$$\left[\frac{\partial^2 \left\langle u'_{iA} u'_{jB}\right\rangle}{\partial X_m \partial X_m}\right]_{\xi=0} = \frac{\partial^2 \left\langle u'_i u'_j\right\rangle}{\partial x_m \partial x_m}. \tag{145}$$

A.1 Pressure–strain fluctuating correlations term

The pressure–strain correlation tensor is defined by

$$\Psi_{ij} = \int_0^\infty \left[\frac{1}{\rho}\left(\frac{\partial}{\partial \xi_i}\left\langle p'_A u'_{jB}\right\rangle - \frac{\partial}{\partial \xi_j}\left\langle p'_B u'_{jA}\right\rangle\right) + \frac{1}{2\rho}\left(\frac{\partial}{\partial X_i}\left\langle p'_A u'_{jB}\right\rangle + \frac{\partial}{\partial X_j}\left\langle p'_B u'_{iA}\right\rangle\right)\right]_{\xi_m=0}^{\Delta} \mathrm{d}\kappa. \tag{146}$$

Using relations (138) and (143), Eq. (146) can be developed and the resulting equation is

$$\Psi_{ij} = \left\langle \frac{p'}{\rho}\left(\frac{\partial u'_i}{\partial x_j} + \frac{\partial u'_j}{\partial x_i}\right)\right\rangle. \tag{147}$$

A.2 Dissipation rate

The dissipation tensor is defined by

$$\epsilon_{ij} = \int_0^\infty \left[\frac{\nu}{2}\frac{\partial^2 \varphi_{ij}}{\partial X_l X_l} + 2\nu\kappa_m^2 \varphi_{ij}\right]_{\xi_m=0} \mathrm{d}\kappa. \tag{148}$$

So that

$$\epsilon_{ij} = \frac{\nu}{2}\left(\frac{\partial^2 R_{ij}}{\partial X_l X_l}\right)_{\xi_m=0} - 2\nu\left[\frac{\partial^2 R_{ij}}{\partial \xi_m \partial \xi_m}\right]_{\xi_m=0}. \tag{149}$$

Using the derivative relations (141), (144) and (145), we can compute easily the terms of the right-hand side of Eq. (149) leading the expected result obtained in one-point closure

$$\epsilon_{ij} = 2\nu\left\langle \frac{\partial u'_i}{\partial x_m}\frac{\partial u'_j}{\partial x_m}\right\rangle. \tag{150}$$

A.3 Diffusion term

The diffusion term J_{ij} is defined by the expression

$$J_{ij} = \int_0^\infty \left[-\frac{1}{\rho} \left(\frac{\partial}{\partial X_i} \left\langle p' u'_{jB} \right\rangle + \frac{\partial}{\partial X_j} \left\langle p' u'_{iA} \right\rangle \right)^\Delta \right]_{\xi_m=0} \mathrm{d}\kappa$$
$$+ \int_0^\infty \left[-\frac{1}{2} \frac{\partial}{\partial X_k} \left(\left\langle u'_{i_A} u'_{k_B} u'_{j_B} \right\rangle^\Delta + \left\langle u'_{i_A} u'_{k_A} u'_{j_B} \right\rangle^\Delta \right) + \nu \frac{\partial^2 \varphi_{ij}}{\partial X_l X_l} \right]_{\xi_m=0} \mathrm{d}\kappa. \tag{151}$$

As for the previous calculus, using (144) and (145) provides the well known result

$$J_{ij} = -\frac{1}{\rho} \left(\frac{\partial}{\partial x_i} \left\langle p' u'_j \right\rangle + \frac{\partial}{\partial x_j} \left\langle p' u'_i \right\rangle \right) - \frac{\partial}{\partial x_k} \left\langle u'_i u'_j u'_k \right\rangle + \nu \frac{\partial^2 R_{ij}}{\partial x_l x_l}. \tag{152}$$

A.4 Transfer term

The total transfer term T_{ij} is defined by

$$T_{ij} = -\int_0^\infty \left[\left(\frac{\partial}{\partial \xi_k} \left[\left\langle u'_{i_A} u'_{k_B} u'_{j_B} \right\rangle - \left\langle u'_{i_A} u'_{k_A} u'_{j_B} \right\rangle \right] \right)^\Delta + \left(\xi_m \frac{\partial R_{ij}}{\partial \xi_k} \right)^\Delta \frac{\partial \langle u_k \rangle}{\partial X_m} \right]_{\xi_m=0} \mathrm{d}\kappa. \tag{153}$$

Obviously, the transfer term T_{ij} is reduced to zero for $\xi_m = 0$ when points A and B go to the midway position X_m.

References

1. Speziale, C.G.: Analytical methods for the development of Reynolds-stress closures in turbulence. Ann. Rev. Fluid Mech. **23**, 107–157 (1991)
2. Speziale, C.G., Sarkar, S., Gatski, T.B.: Modelling the pressure–strain correlation of turbulence: an invariant dynamical systems approach. J. Fluid Mech. **227**, 245–272 (1991)
3. Launder, B.E.: Second moment closure: Present and future? Int. Heat Fluid Flow **20**(4), 282–300 (1989)
4. Hanjalic, K., Launder, B.E., Schiestel, R.: Multiple time-scale concepts in turbulence transport modeling. In: Turbulent Shear Flows, 2nd edn. Springer (1980)
5. Schiestel, R.: Multiple-time scale modeling of turbulent flows in one point closures. Phys. Fluids **30**(3), 722–731 (1987)
6. Lesieur, M., Métais, O.: New trends in large-eddy simulations of turbulence. Ann. Rev. J. Fluid Mech. **28**, 45–82 (1996)
7. Chaouat, B.: Simulations of channel flows with effects of spanwise rotation or wall injection using a Reynolds stress model. J. Fluid Eng. ASME, **123**, 2–10 (2001)
8. Chaouat, B.: Reynolds stress transport modeling for high-lift airfoil flows. AIAA J. **44**(10), 2390–2403 (2006)
9. Leschziner, M.A., Drikakis, D.: Turbulence modelling and turbulent-flow computation in aeronautics. Aeronaut. J. **106**, 349–384 (2002)
10. Rumsey, C.L., Gatski, T.B.: Recent turbulence model advances applied to multielement airfoil computations. J. Aircraft, **38**(5), 904–910 (2001)
11. Lesieur, M., Métais, O., Comte, P.: Large-Eddy Simulations of Turbulence. Cambridge University Press, (2005)
12. Spalart, P.R.: Strategies for turbulence modelling and simulations. Int. J. Heat Fluid Flow **21**, 252–263 (2000)
13. Hamba, F.: An attempt to combine large eddy simulation with the $k-\epsilon$ model in a channel-flow calculation. Theoret. Comput. Fluid Dyn. **14**, 323–336 (2001)
14. Hamba, F.: A hybrid RANS/LES simulation of turbulent channel flow. Theoret. Comput. Fluid Dyn. **16**, 387–403 (2003)
15. Temmerman, L., Hadziabdic, M., Leschziner, M.A., Hanjalic, K.: A hybrid two-layer URANS-LES approach for large eddy simulation at high reynolds numbers. Int. J. Heat Fluid Flow **26**, 173–190 (2005)
16. Schiestel, R., Dejoan, A.: Towards a new partially integrated transport model for coarse grid and unsteady turbulent flow dimulations. Theoret. Comput. Fluid Dyn. **18**, 443–468 (2005)
17. Chaouat, B., Schiestel, R.: A new partially integrated transport model for subgrid-scale stresses and dissipation rate for turbulent developing flows. Phys. Fluids **17**(6), (2005)
18. Chaouat, B., Schiestel, R.: Progress in subgrid-scale transport modeling using partial integration method for LES of developing turbulent flows. In: Lamballais, E., Friedrich, R., Geurts, B., Métais, O. (eds) Direct and Large eddy Simulation VI, Ercoftac Series, Vol. 10, Springer (2006)

19. Germano, M.: From RANS to DNS: toward a bridging model. In: Voke, P., Sandham, N.D., Kleiser, L. (eds) Direct and Large-Eddy simulation III, Ercoftac Series, Vol. 7 pp. 225-235. Kluwer (1999)
20. Hanjalic, K., Hadziabdic, M., Temmerman, M., Leschziner, M.: Merging LES and RANS strategies: zonal or seamless coupling ? In: Friedrich, R., Geurts, B., Métais, O. (eds.) Direct and Large-Eddy simulation V, Ercoftac Series Vol. 9, pp. 451–464, Kluwer, Dordrecht (2004)
21. Cambon, C., Jeandel, D., Mathieu, J.: Spectral modelling of homogeneous non-isotropic turbulence. J. Fluid Mech. **104**, 247–262 (1981)
22. Burden, A.D.: Toward an EDQNM-closure for inhomogeneous turbulence. In: Johansson, A.V., Alfredson, P.H. (eds) Advances in Turbulence III, Proceeding of the third European Turbulence Conference Stockholm, pp. 387–394. Springer, (1991)
23. Besnard, D.C., Harlow, F.H., Rauenzahn, R.M., Zemach, C.: Spectral transport model for turbulence. Theoret. Comput. Fluid Dyn. **8**, 1–35 (1996)
24. Laporta, A.: Etude spectrale et modélisation de la turbulence inhomogène. PhD thesis, Ecole Centrale Lyon, (1995)
25. Laporta, A., Bertoglio, J.P.: A model for inhomogeneous turbulence based on two-point correlations. In: Benzi, R. (ed) Advances in Turbulence V, pp. 286–297. Kluwer (1995)
26. Bertoglio, J.P., Jeandel, D.: A simplified spectral closure for inhomogeneous turbulence: application to the boundary layer. In: 5th Symposium on Turbulence Shear Flows, Springer, Corneil Univ., (1986)
27. Parpais, S.: Développement d'un modèle spectral pour la turbulence inhomogène; Résolution par une méthode d'élements finis. PhD thesis, Ecole Centrale Lyon, (1997)
28. Touil, H., Bertoglio, J.P., Parpais, S.: A spectral closure applied to anisotropic inhomogeneous turbulence. In: Dopazo et al. C. (eds) Advances in Turbulence VIII, Proceeding Hight European Turbulence Conference Barcelona, pp. 689–692 (2000)
29. Touil, H.: Modélisation spectrale de la turbulence inhomogène anisotrope. PhD thesis, Ecole Centrale Lyon, (2002)
30. Clark, T.T., Zemach, C.: A spectral model applied to homogeneous turbulence. Phys. Fluids, **7**(7), 1674–1694 (1995)
31. Rubinstein, R., Clark, T.T.: A generalized Heisenberg model for turbulent spectral dynamics. Theoret. Comput. Fluid Dyn. **17**, 249–272 (2004)
32. Yoshizawa, A.: Statistical analysis of the deviation of the Reynolds stress form its eddy-viscosity representation. Phys. Fluids, **27**(6), 1377–1387 (1984)
33. Godeferd, F.S., Cambon, C., Scott, J.F.: Two-point closures and their applications: report on a workshop. J. Fluid Mech. **436**, 393–407 (2001)
34. Schiestel, R.: Sur le concept d'échelles multiples en modélisation des écoulements turbulents. part I. J. Mécanique Théorique Appl. **2**(3), 417–449 (1983)
35. Schiestel, R.: Sur le concept d'échelles multiples en modélisation des écoulements turbulents. part II. J. Mécanique Théorique Appl. **2**(4), 601–628 (1983)
36. Cadiou, A., Hanjalic, K., Stawiarski, K.: A two-scale second-moment turbulence closure based on weighted spectrum integration. Theoret. Comput. Fluid Dyn. **18**, 1–26 (2004)
37. Liu, N.S., Shih, T.H.: Turbulence modeling for very large-eddy simulation. AIAA J. **44**(4), 687–697 (2006)
38. Bhushan, S., Warsi, Z.U.A.: Large eddy simulation of turbulent channel flow using an algebraic model. Int. J. Numer. Methods Fluids **49**, 489–519 (2005)
39. Bhushan, S., Warsi, Z.U.A., Walters, D.K.: Modeling of energy backscatter via an algebraic subgrid-stress model. AIAA J. **44**(4), 837–847 (2006)
40. Jeandel, D., Brison, J.F., Mathieu, J.: Modeling methods in physical and spectral space. Phys. Fluids **21**(2), 169–182 (1978)
41. Schiestel, R., Elena, L.: Modeling of anisotropic turbulence in rapid rotation. Aerosp. Sci. Technol. **7**, 441–451 (1997)
42. Yoshizawa, A.: A statistically-derived subgrid model for the large-eddy simulation of turbulence. Phys. Fluids **25**(9), 1532–1538 (1982)
43. Germano, M.: A statistical formulation of the dynamic model. Phys. Fluids **8**(2), 565–570 (1996)
44. Hinze, J.O.: Turbulence. Mc. Graw-Hill (1975)
45. Schiestel, R.: Méthodes de modélisation et de simulation des écoulements turbulents. Hermès-Lavoisier, (2006)
46. Jones, W.P., Launder, B.E.: The prediction of laminarization with a two-equation model of turbulence. Int. J. Heat Mass Transf. **15**, 301–314 (1972)
47. Jovanovic, J., Ye, Q.Y., Durst, F.: Statistical interpretation of the turbulent dissipation rate in wall-bounded flows. J. Fluid Mech. **293**, 321–347 (1995)
48. Jakirlic, S., Hanjalic, K.: A new approach to modelling near-wall turbulence energy and stress dissipation. J. Fluid Mech. **459**, 139–166 (2002)
49. Launder, B.E., Reece, G.J., Rodi, W.: Progress in the development of a Reynolds stress turbulence closure. J. Fluid Mech. **68**, 537–566 (1975)
50. Hanjalic, K.: Advanced turbulence closure models: A view of current status and future prospects. Int. J. Heat Fluid Flow **15**(3), 178–203 (1994)
51. Germano, M.: Turbulence: the filtering approach. J. Fluid Mech. **238**, 325–336 (1992)
52. Rubinstein, R., Zhou, Ye.: Analytical theory of the destruction terms in the dissipation rate transport equation. Phys. Fluids **8**(11), 3172–3178 (1996)
53. Rubinstein, R., Zhou, Ye.: Schiestel's derivation of the epsilon equation and two equations modelling or rotating turbulence. Technical report, NASA, 2001. NASA/CR n° 2001-21 1060, ICASE Report n° 2001-24
54. Rubinstein, R., Clark, T.T., Livescu, D., Li-Shi Luo. Time-dependent isotropic turbulence. J. Turbul. 5, (2004)
55. Rogallo, R.S.: Numerical experiments in homogeneous turbulence. In Proc. Conf. on Computational of Complex Turbulent Flows, Stanford Univ. Calif., (1981)
56. Uberoi, M.S., Wallis, S.: Small axisymmetric contraction of grid turbulence. J. Fluid Mech. **24**, 539–543 (1966)
57. Lee, M.J., Reynolds, W.C.: Numerical experiments on the structure of homogeneous turbulence. Technical report, Stanford University, 1985. report n° TF-24, Department of mechanical Engineering

58. Comte-Bellot, G., Corrsin, S.: Simple Eulerian time correlation of full and narrow-band velocity signals in grid-generated, isotropic turbulence. J. Fluid Mech. **48**, 273–337 (1971)
59. Schiestel, R.: Sur la modélisation des écoulements en non-équilibre spectral. C. R. Acad. Sci. Paris **302**(11), 727–730 (1986)
60. Launder, B.E., Sharma, B.I.: Application of the energy dissipation model of turbulence to the calculation of flow near a spinning disc. Lett. Heat Mass Transf. **1**, 131–138 (1974)
61. Binder, G., Kuény, G.: Measurements of the periodic oscillations near the wall in unsteady turbulent channel flow. Unsteady turbulent shear flows. IUTAM Symp. pp. 100–109, Springer, Heidelberg (1981)
62. Tardu, S., Binder, G., Blackwelder, R.: Turbulent channel flow with large amplitude velocity oscillations. J. Fluid Mech. **267**, 109–151 (1994)
63. Launder, B.E., Shima, N.: Second moment closure for the near wall sublayer: Development and application. AIAA J. **27**(10), 1319–1325 (1989)
64. Gany, A., Aharon, I.: Internal ballistics considerations of nozzleless rocket motors. J. Propul. Power **15**(6), 866–873 (1999)
65. Chaouat, B., Schiestel, R.: Reynolds stress transport modelling for steady and unsteady channel flows with wall injection. J. Turbul. **3**, 1–15 (2002)
66. Germano, M., Piomelli, U., Moin, P., Cabot, W.H.: A dynamic subgrid-scale eddy-viscosity model. Phys. Fluids **3**(7), 1760–1765 (1992)
67. Wasistho, B., Moser, R.D.: Simulation strategy of turbulent internal flow in solid rocket motor. J. Propul. Power **21**(2), 251–263 (2005)
68. Apte, S.A., Yang, V.: A large-eddy simulation study of transition and flow instability in a porous-walled chamber with mass injection. J. Fluid Mech. **477**, 215–225 (2003)
69. Chaouat, B.: Numerical predictions of channel flows with fluid injection using Reynolds stress model. J. Propul. Power **18**(2), 295–303 (2002)
70. Avalon, G., Casalis, G., Griffond, J.: Flow instabilities and acoustic resonance of channels with wall injection. AIAA Paper 98–3218, July (1998)